Palaeogeography, Palaeoclimatology, Palaeoecology xxx (xxxx) 111450

Contents lists available at ScienceDirect

Palaeogeography, Palaeoclimatology, Palaeoecology

journal homepage: www.elsevier.com/locate/palaeo

Planktonic foraminifera response to orbital and millennial-scale climate variability at the southern Iberian Margin (IODP Site U1385) during Marine Isotope Stages 20 and 19

Angela Girone [a,*], Adriano De Astis [a], Francisco J. Sierro [b], Ivan Hernández-Almeida [c], Montserrat Alonso Garcia [b], Maria F. Sánchez Goñi [d,e], Patrizia Maiorano [a], Maria Marino [a], Samanta Trotta [a], David Hodell [f]

[a] Dipartimento di Scienze della Terra e Geoambientali, Università di Bari Aldo Moro, via E. Orabona 4, 70125 Bari, Italy
[b] Department of Geology, Faculty of Sciences, University of Salamanca, 37008 Salamanca, Spain
[c] Swiss Federal Institute of Technology in Zurich (ETHZ), Department of Earth Sciences, Zurich, Switzerland
[d] Ecole Pratique des Hautes Etudes (EPHE, PSL University), 75014 Paris, France
[e] University of Bordeaux, EPOC, UMR 5805, F-33615 Pessac, France
[f] Godwin Laboratory for Palaeoclimate Research, Department of Earth Sciences, University of Cambridge, UK

ARTICLE INFO

Editor: Prof. M Elliot

Keywords:
North Atlantic
Termination IX
Millennial-scale SST
Planktonic foraminifera

ABSTRACT

The orbital configuration of Marine Isotope Stage (MIS) 19 provides a good analogue to our present interglacial, and it is marked by millennial-scale climate variability. To evaluate how orbital and millennial-scale climate changes interact during this interglacial we have conducted a high-resolution study of planktonic foraminifera assemblages at International Ocean Discovery Program (IODP) Site U1385, SW Iberian Margin, encompassing late MIS 20 and MIS 19. Estimates of sea surface temperature (SST), using transfer-functions, are compared with geochemical, XRF elemental data, biomarker and pollen records from the same site. These results are then compared with SST and ice-rafted debris records from North Atlantic IODP Site U1314 to reconstruct basin-wide palaeoceanographic conditions. During MIS 20, the large size of the ice sheets imparted a strong cooling in the subpolar gyre whereas the Iberian Margin remained under the influence of the subtropical gyre with the development of a high meridional thermal gradient in the North Atlantic. During MIS 20 terminal stadial (794–789 ka) and MIS 19b-a stadial events, the meltwater discharges related to the instability of ice sheets affected both the North Atlantic and the Iberian Margin leading to a weaker thermal gradient. Our data indicate that Termination IX (TIX, ~795–788 ka) was punctuated by short-term warming/cooling phases in the ocean coupled with warming/cooling events on land. A short-term cooling episode, recognized in the ocean and on land, occurred on Termination IX and preceded the beginning of MIS 19c. During MIS 19c, the planktonic foraminifera SST indicates warm and almost stable conditions in the sea decoupling the cool and dry millennial-scale events on land inferred by pollen assemblages. Starting from 780 ka towards MIS 18, the planktonic foraminifera assemblages and SSTs indicate a cooling trend along the Iberian Margin related to a progressive southward migration of the polar front.

1. Introduction

Marine Isotope Stage (MIS) 19 has received much attention in studies of interglacial climate variability because it is considered a good analogue for MIS 1 in terms of orbital configuration (Tzedakis et al., 2009, 2012a, 2012b; Pol et al., 2010; Yin and Berger, 2012, 2015; Ferretti et al., 2015; Giaccio et al., 2015). The orbital configurations of both MIS 19 and MIS 1 are characterized by a weak eccentricity-precession forcing, which results in a subdued amplitude of insolation changes (Yin and Berger, 2012, 2015). Millennial-scale climate variability during Pleistocene interglacials is also of interest because of its potential to provide information about climate stability or instability during the Holocene. Several studies carried out in European lacustrine sediments (Giaccio et al., 2015; Wagner et al., 2019) and in marine suc-

* Corresponding author.
E-mail address: angela.girone@uniba.it (A. Girone).

https://doi.org/10.1016/j.palaeo.2023.111450
Received 22 September 2022; Received in revised form 21 January 2023; Accepted 8 February 2023
0031-0182/© 20XX

cessions from central and western Mediterranean area (Bertini et al., 2015; Marino et al., 2015; Maiorano et al., 2016; Nomade et al., 2019; Quivelli et al., 2021; Marino et al., 2020) have also highlighted the strong similarity between Termination I (TI) and Termination IX (TIX) and their relationship with the North Atlantic climate oscillations.

In the North Atlantic, millennial-scale climate oscillations occurring during Pleistocene interglacials have been linked to oceanic and atmospheric processes related to ice sheet instability (McAyeal, 1993; Marcott et al., 2011). Associated with iceberg-discharge events, several extreme cooling events have been recorded by drops in SST and decreases in log (Ca/Ti) (Martrat et al., 2007; Rodrigues et al., 2011; Voelker and de Abreu, 2013; Martin-Garcia et al., 2015; Hodell et al., 2013, 2015; Rodrigues et al., 2017). These events have punctuated both interglacial and glacial periods, but with greater amplitude at glacial onsets and terminations (Hodell et al., 2022) and are associated with a strong reduction of the Atlantic Meridional Overturning Circulation (AMOC) and a southern shift of the Subpolar Front (Hodell et al., 2013, 2015, 2022; Rodrigues et al., 2017). Pronounced cooling occurred at TIX as recorded by low alkenone-based SST, which is followed by a large increase in SST towards peak interglacial conditions of MIS 19c (increase of 10 °C within 2.5 ka) (Rodrigues et al., 2017).

Interglacial MIS 19 has been marked by millennial-scale climate changes with a repeat time of ~5000 years (Ferretti et al., 2015; Sánchez Goñi et al., 2016). The millennial climate variability (MCV) in the mid- and high- latitude North Atlantic may be triggered by precession-forced low latitude dynamics related to harmonics of precession (Berger et al., 2006; Ferretti et al., 2010; Hernandez-Almeida et al., 2012; Ferretti et al., 2015; Sánchez Goñi et al., 2016) that influenced the North Atlantic latitudinal thermal gradient and the northward transport of heat and water vapor from equatorial regions. The increased transport of moisture to the northern high latitudes could have contributed to ice sheet growth during the onset of glacial conditions at the start of MIS 18 (Sánchez Goñi et al., 2016).

At Site U1385, the existing low-resolution planktonic foraminifera analyses for the time interval including MIS20 and MIS19 did not explore the millennial-scale variability and focused on long-term palaeoceanographic changes in the North Atlantic circulation during the Middle Pleistocene Transition (Martin-Garcia et al., 2015, 2018; Bahr et al., 2018). Here we present new higher resolution records of planktonic foraminifera assemblages and seasonal and annual foraminifera-based SST (Sea Surface Temperature) at orbital and millennial-scale to reconstruct sea-surface and subsurface dynamics during late MIS 20-MIS 19 at IODP Site U1385 and their relationship with Northern Hemisphere high latitude ocean-atmosphere dynamics. The study aims to provide insights into i) the late MIS 20 terminal stadial and its oceanographic-atmospheric connection with North Atlantic climate, ii) the high-frequency climate variability across the deglaciation associated with TIX. Moreover, starting from the previously published studies focused on the pollen-based atmospheric processes associated with changes in the marine realm (Hodell et al., 2015; Sánchez Goñi et al., 2016; Rodrigues et al., 2017), our data have been directly compared with the same resolution pollen and isotopic record available at the Site U1385 (Sánchez Goñi et al., 2016) in order to evaluate the effects of land-ocean interactions at millennial scale during the studied interval. The overarching aim of the study is to test whether the observed millennial-scale air-sea temperature decoupling based on pollen-alkenone-based SST (Sánchez Goñi et al., 2016) is also recorded by the planktonic foraminifera assemblages. Planktonic foraminifera are among the most widely used proxies for paleoceanographic and paleoclimate sea-surface reconstructions. Their distribution and abundance are strongly linked to surface water properties, and they represent a good tool to trace the variations of water masses because each water mass is characterized by distinct physical–chemical parameters and specific planktonic foraminiferal assemblages (e.g. Bé, 1977; Ottens, 1991; Cayre et al., 1999). In addition, the distribution of planktonic foraminifera is strictly related to the sea surface temperatures and to other environmental parameters, such as food availability, light intensity, interspecific competition, and salinity (Bé and Tolderlund, 1971; Bé, 1977; Hemleben et al., 1989). Those environmental parameters may be directly influenced by the atmospheric processes, particularly the variations in the mixed layer.

The Iberian Margin is very sensitive to variations in North Atlantic atmospheric processes and its oceanographic setting is influenced by changes in the northeastward transport of the different branches of the North Atlantic Current (NAC) towards the European continental margin. Changes in the intensity of the NAC influence the North Atlantic subpolar and subtropical gyres, as well as the position of the Arctic and Subtropical Fronts. Moreover, it is the main driver of the transport of warm, salty surface water from tropical regions to the polar ocean and is responsible for the transfer of heat and moisture to the atmosphere, which can feed the growth of polar ice sheets (e.g. McCartney and Talley, 1982; Ruddiman and McIntyre, 1984; Schmitz and McCartney, 1993; Rahmstorf, 1995; Chapman and Maslin, 1999). To better understand such dynamics during late MIS 20, TIX and MIS 19, the data at Site U1385 have been compared with published (distribution pattern of planktonic foraminifera, isotope stratigraphy) (Alonso-Garcia et al., 2011a, 2011b; Hernández-Almeida et al., 2013, 2015) and unpublished data (seasonal foraminifera-based SST) from IODP Site U1314 located at higher latitude on the Gardar Drift to south of Iceland. The study also benefits from the comparison with the available U1385 XRF elemental data (Hodell et al., 2015) and the biomarker record at the same site (Rodrigues et al., 2017).

2. Material and methods

2.1. Site location and oceanographic setting

IODP Site U1385 was drilled at the "Shackleton site" off the western Iberian Margin (37°34.284′N, 10°7.562′W), at 2578 m water depth (Fig. 1). The studied sedimentary section mainly consists of nannofossil muds and nannofossil clays (Expedition 339 Scientists, 2013), with an average sedimentation rates of ~11 cm/kyr (Hodell et al., 2015). The stratigraphy of IODP Site U1385 was built upon a combination of chemo-stratigraphic measurements. Core scanning XRF (X-ray fluorescence) was used to measure Ca/Ti of sediment every cm in all holes to define a composite section (Hodell et al., 2015). In this study, we use the high-resolution (every 2 cm) benthic and planktonic oxygen isotope stratigraphy reported in Sánchez Goñi et al. (2016) plotted against the age model obtained by the correlation of the $\delta^{18}O_b$ to the LR04 stack (Hodell et al., 2013, 2015). Transitions between the different Marine Isotopic Stages (MIS) and sub-stages are defined in Sánchez Goñi et al. (2016) based on significant shifts in the $\delta\ ^{18}O_b$ record (Fig. 2).

Site U1385 (Fig. 1) is currently under the influence of Eastern North Atlantic Central Water (ENACW) at the surface and North Atlantic Deep Water (NADW) at the sea floor. The main surface currents are the Portugal Current (PC) and Azores Current (AzC) (Fig. 1). The PC forms in the Northeastern Atlantic (McCartney and Talley, 1982) as a branch of the North Atlantic Current and brings cold, nutrient-rich water southward along the Iberian Margin from 45° to 30°N (Peliz et al., 2005). The subsurface component of PC is the subpolar Eastern North Atlantic Central Water (ENACWsp) (Peliz et al., 2005). The AzC (Fig. 1) is an eastward flowing current that diverges from the Gulf Stream and moves in large meanders between 35° and 37°N. The AzC is characterized by cyclonic recirculation to the north of the Azores Front and anti-cyclonic recirculation to the south (Gould, 1985; Käse and Siedler, 1982; Pingree, 1997; Pingree and Sinha, 1998). In the eastern basin the AzC divides into several branches of which Canary Current (CC) is the major southward recirculation branch (Fig. 1). An eastward branch enters in the Gulf of Cadiz (Fig. 1). During winter, the Iberian Poleward Current (IPC) originates as northward recirculation waters of this eastern

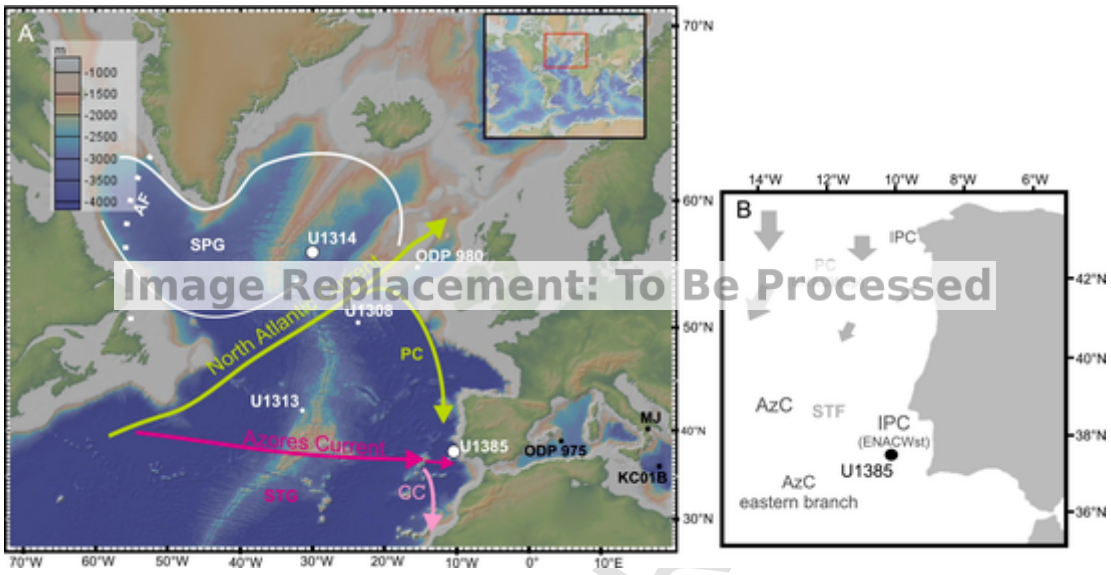

Fig. 1. A: Modern surface circulation in the North Atlantic and location of the sites discussed in the text. B: Winter surface and subsurface circulation scheme off Portugal after Peliz et al. (2005); modified from Voelker et al. (2010). PC: Portugal Current; IPC: Iberian Poleward Current; ENACWsp: Eastern North Atlantic Central Waters of subpolar origin; ENACWst: Eastern North Atlantic Central Water of subtropical origin; SPG: Subpolar Gyre; STG: Subtropical Gyre; STF: Subtropical Front; AzC: Azores Current; AF: Artic Front; CC: Canary Current. Map source http://www.geomapapp.org/.

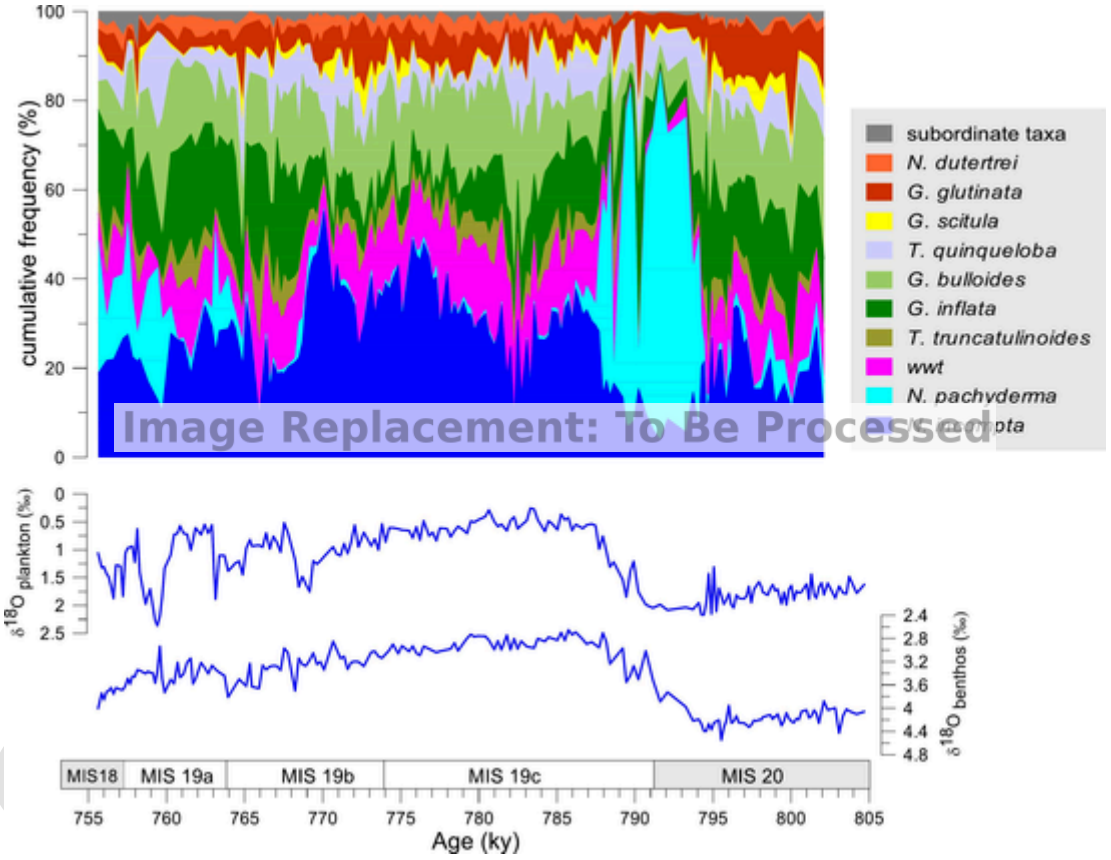

Fig. 2. Cumulative abundances of planktonic foraminifera at IODP Site U1385 plotted against the $\delta^{18}O$ plankton and $\delta^{18}O$ benthos (Hodell et al., 2015; Sánchez Goñi et al., 2016) vs age.

branch (Peliz et al., 2005) moving the subtropical front along the western Iberian margin. IPC is composed of subsurface less ventilated, nutrient-poor, warm and saltier waters of subtropical origin (Eastern North Atlantic Central Water, ENACWst) (Frouin et al., 1990; Haynes and Barton, 1990) (Fig. 1). The northern boundary of the AzC forms the Subtropical Front (STF). The surface and subsurface circulation is influenced by the atmospheric pressure gradients related to intensity and relative position of Azores High and Iceland Low atmospheric pressure cells and by the associated large-scale wind pattern (Barton et al., 2001; Fiúza et al., 1998; Relvas et al., 2007). During the late spring and sum-

mer months, the northward displacement and strengthening of the Azores high pressure cell and strong northerly winds generate coastal upwelling and a relatively cold, nutrient-rich water band forms along the western coast (Fiúza et al., 1982; Fiúza, 1984; Sousa and Bricaud, 1992; Sánchez and Relvas, 2003). The waters involved in the upwelling system are ENACW, either of subpolar or subtropical origin (Sánchez and Relvas, 2003). During the winter, when the Azores high weakens, the surface circulation reverses and a northward flow of warm and saline surface water reaches higher latitudes offshore Portugal (Fiúza et al., 1998; Peliz et al., 2005).

2.2. Planktonic foraminifera study

Quantitative analyses of planktonic foraminifera assemblages were performed on 160 samples with a spacing of 2 cm, corresponding to an average time resolution of ~250 yr according to the age model of Hodell et al. (2015). This study includes the stratigraphic section between 93.35 and 88.91 corrected meter composite depth (crmcd), which encompasses late MIS 20 and the beginning of MIS 18 (Fig. 2).

Samples were washed through a 63 μm sieve and dried. The > 63 μm residue was dried and sieved again to separate the >150 μm fraction. These residues were split until a representative aliquot containing about 300 specimens was obtained. All specimens were counted in each aliquot and species abundances were quantified as percentages of the total number of planktonic foraminifers. Twenty-one species or species groups were distinguished. To obtain consistency with foraminiferal counts produced by other researchers, *Trilobatus sacculifer* includes *Trilobatus trilobus* and *Trilobatus quadrilobatus* (sensu Hemleben et al., 1989; André et al., 2013; Spezzaferri et al., 2015). *Neogloboquadrina incompta* corresponds to those specimens previously referred to as *Neogloboquadrina pachyderma* (dextral) and includes intergradations between *N. pachyderma* (dextral) and *Neogloboquadrina dutertrei* (Darling et al., 2006). *N. pachyderma* only includes the left coiling specimens. In our record *Truncorotalia truncatulinoides* is represented by dextral tests only in agreement with the evidence of a pronounced absence of sinistral coiling specimens during the time interval between MIS 21 and MIS 15 (Kaiser et al., 2019) in the North Atlantic.

The analyses of planktonic foraminifera focused on species that are associated with North Atlantic surface water masses and with the southern Iberian Margin surface waters. *Globigerinoides ruber* is the most abundant species within the Subtropical Gyre (STG) (Ottens, 1991; Schiebel et al., 2002a, 2002b) and *T. truncatulinoides* is the most abundant species south of Azores Front (AzF) (Ottens, 1991; Schiebel et al., 2002a, 2002b). Both are used to trace the influence of subtropical waters at the site location and the strength of AzC and STG. *G. bulloides* is used as indicator of nutrient-rich conditions related to upwelling conditions in accordance with the findings of Vautravers and Shackleton (2006) and Salgueiro et al. (2008). *N. incompta* and *G. inflata* are reported as the main taxa associated with the PC (Salgueiro et al., 2008; Ottens, 1991). Following its preference for colder conditions, *N. incompta* is generally more abundant along the coast of the Iberian Margin, north of 39°N where the temperatures are lower than those to the south (Salgueiro et al., 2008). In this study, *N. incompta* is used to trace colder, nutrient-rich waters associated with the PC along the Iberian Margin and at the site location (Salgueiro et al., 2008). *G. inflata*, a transitional water taxon (Giraudeau, 1993) and often associated to hydrologic fronts (Rohling et al., 1995), is used to evaluate the influence of temperate and oligotrophic transitional water because it occurs in the region influenced by ENACWst along the Iberian Margin (Salgueiro et al., 2008). *N. pachyderma* is used to trace the presence of polar water masses (Cayre et al., 1999; Pflaumann et al., 2003; Eynaud et al., 2009) whereas *Turborotalita quinqueloba*, usually associated with the Artic Front (AF) (Johannessen et al., 1994; Cayre et al., 1999), is a characteristic species of spring blooms and upwelling stages (Weaver and Pujol, 1988; Sautter and Sancetta, 1992; Schiebel et al., 2004). The latter species also proliferate in areas marked by highly fertile, low-density surface waters (Aksu et al., 2002; Hemleben et al., 1985; Pujol and Vergnaud-Grazzini, 1995; Triantaphyllou et al., 2010) and those influenced by continental runoff (Rohling et al., 1997; Jonkers et al., 2010; Girone et al., 2013; Bartels-Jónsdóttir et al., 2015; Margaritelli et al., 2016). Warm-water taxa (wwt) (Vautravers et al., 2004) include all species dwelling in tropical-subtropical water masses such as *G. ruber*, *T. sacculifer*, *Globoturborotalita rubescens*, *Globoturborotalita tenella*, *Orbulina universa*, *Globigerinella siphonifera*, *Beella digitata*, *Globigerina falconensis* and *Pulleniatina obliquiloculata*.

2.3. Transfer function and SST reconstruction

We used the fossil planktonic foraminifera assemblages to reconstruct the temperatures for the studied interval. Although temperatures for U1314 had been reconstructed previously using this approach for the interval MIS 31–11 (Alonso-Garcia et al., 2011a; Hernandez-Almeida et al., 2012), we re-analyzed the planktonic-foraminifera-based SST estimates at this site and at U1385 using the same methodology for both and the most recent calibration datasets for consistency.

For the development of the transfer function, we used the core-top planktonic foraminifera assemblage dataset from the North Atlantic from the ForCens compilation (Siccha and Kucera, 2017). Seasonal and annual ocean temperatures at different depths were interpolated for the core top location and extracted from the World Ocean Atlas 2001 (WOA01) (Conkright et al., 2002) at 10 and 200 m for spring, winter and annual conditions. We include the 200 m depth because it has been shown that fossil planktonic foraminifera assemblages in the North Atlantic are more sensitive to subsurface temperatures at some locations than to 10 m SST (Telford et al., 2013). We applied the resulting transfer function to the fossil planktonic foraminifera assemblages from Sites U1385 and U1314. The taxonomy of the fossil samples was harmonized according to the ForCenS database, following criteria suggested by Siccha and Kucera (2017).

The modern analogue technique (MAT) (Prell, 1985) is a widely used regression method in paleoceanographic reconstructions. This approach identifies a subset of samples in the calibration data set using similarity measures to reconstruct quantitatively the environmental variable of interest. We selected the optimal number of close analogues determined using squared chord distance (Prell, 1985). The performance of the resulting models, coefficient of determination (R^2) and root mean square of prediction (RMSEP), were assessed using cross validation (bootstrapping, 999 permutation cycles) (Vaughan and Ormerod, 2005), with a cut-off distance of 850 km to account for the effect of spatial autocorrelation in the modern dataset (Telford and Birks, 2009), following recommendation from other studies in the North Atlantic (Trachsel and Telford, 2016). Similarity between the modern and the fossil dataset was evaluated by calculating the chord distance between them (analogue quality) (Overpeck et al., 1985). To evaluate whether temperature at each depth and season were also significant for the downcore assemblage at Sites U1385 and U1314, we used the statistical test developed by Telford and Birks (2011). This method compares the variance in the fossil assemblage explained by the environmental variable of interest with the proportion of variance explained by randomly generated environmental variables. Transfer function development and downcore reconstructions at each depth were performed in R (R core team, 2020) using the packages rioja (Juggins, 2017), raster (Hijmans, 2017), vegan (Oksanen et al., 2018), ggpalaeo (Telford, 2019), and ggplot2 (Wickham, 2016).

3. Results

3.1. Planktonic foraminifera assemblages

Planktonic foraminifera at Site U1385 are well preserved and diversified across the studied interval. The assemblages are mainly represented by *N. incompta* that occurs throughout the entire studied interval showing the highest percentages between ~780 ka and ~ 769 ka (Fig. 2). *N. pachyderma* has a more scattered distribution showing good correspondence to the polar-index % $C_{37:4}$ of Site U1385 (Rodrigues et al., 2017); it occurs during late MIS 20 and late MIS 19 associated with the millennial-scale cooling events during the transition to MIS 18. During late MIS 20 it represents up to 80% of the total assemblage (Fig. 2). *N. dutertrei* is also found along the entire studied section except for the late MIS 20 terminal stadial event (794–789 ka). It occurs with very low percentages never exceeding 8% of the total assemblage. The wwt group shows highest abundance during MIS 19c and interstadials of MIS 19 b-a (774–771 ka; 768.7–765.3 ka; 762.9–760.3 ka). The lowest abundances of this group are recorded during the terminal stadial event of MIS 20 (Fig. 2). *T. truncatulinoides* occurs frequently and its pattern follows that of the wwt group trend. *Globigerina bulloides* and *T. quinqueloba* are distributed through the entire section: *G. bulloides* shows values ranging between 15% and about 30%. During the MIS 20 terminal stadial event, its values drop below 15% of the total assemblage. *T. quinqueloba* has an average abundance of about 10%, with intervals of maximum relative abundance during the stadial late MIS 19 and between 782 and 784 ka, during MIS 19c. *G. inflata* also contributes about 30% to the total assemblage: it has the lowest abundance values during the MIS 20 terminal stadial event and between 780 ka and 769 ka, during MIS 19. The rest of the assemblage is composed of *Globigerinita glutinata*, *Globorotalia scitula* and *N. dutertrei* that combined represent <20% of the total assemblages. Among these, *G. scitula* is the most abundant with the highest values recorded during the oldest portion of the investigated interval and during MIS 19b. Other less abundant taxa (subordinate taxa in Fig. 2) include *Globigerina falconensis*, *Globorotalia crassaformis* and *P. obliquiloculata*. *G. falconensis* occurs through the entire studied section but generally at very low percentages (lower than 2%), only occasionally showing short-term increases up to 6–7%. The distribution of *G. crassaformis* and *P. obliquiloculata* is very scattered with abundance values lower than 2%. *G. crassaformis* has a more continuous distribution during MIS 20 (with exception of the terminal stadial) and the early interval of MIS 19c.

3.2. Faunal-based sea surface temperatures

The performance of the MAT regression with five analogues (MAT-K5) for spring, winter and annual temperatures at surface mixed layer (10 m depth) and subsurface sea water (200 m depth) using the North Atlantic samples from the ForCens database (Siccha and Kucera, 2017) is shown in supplementary Table 1. The cross-validated R^2 of all the models is above 0.95, and the RMSEP is between 0.99 and 1.2 °C. The analogue measurements between the modern and fossil samples at Site U1314 show that they are very similar (Supplementary Fig. 1). For samples at Site U1385, only nine samples between 784 and 782 ka and 766–761 ka show poor analogue conditions (Supplementary Fig. 1). The reconstructions for each season and water depth are highly significant ($p < 0.05$), explaining more variance than the randomly generated environmental variables, and thus they can be considered as important environmental factors driving the planktonic foraminifera assemblages in these two cores for the analyzed interval (Supplementary Fig. 2).

At Site U1385, the annual and seasonal SST records show a general trend that is very similar to the log (Ca/Ti) and alkenone-based SST profiles (Fig. 3). The lowest sea surface and subsurface temperatures are recorded during the MIS 20 terminal stadial event and during the cold events during MIS 19 b-a associated with the onset of glacial conditions (Fig. 3e-g). During the MIS 20 terminal stadial event, winter surface and subsurface SSTs show very similar values with a minimum of about 4 °C; during spring season such minima values are registered at the subsurface waters while at surface waters the temperatures are close to 5 °C. During TIX, two main warming episodes are recorded in both annual and seasonal temperatures that are marked by increases of up to 8 °C in SST (Fig. 3e-g). Starting at 787.5 ka and continuing throughout the full interglacial MIS 19c, the temperatures were warm with an average SST of ~15 °C in the spring and of ~13 °C in the winter. During MIS 19c, the foraminifera SSTs show oscillations in contrast to the relatively stable log (Ca/Ti) and alkenone-based SST records. The major oscillation, occurring at about 784.5 ka, is marked by a temperature drop of about 5 °C (Fig. 3e-g).

At Site U1314, late MIS 20 is characterized by much lower foraminifera-based temperatures with respect to the Iberian Margin (Fig. 3h-i). Such cold conditions are also recorded in the older interval of MIS 20 terminal stadial but at about 790 ka the SST records indicate a temperature increase of about 7 °C that remained high throughout TIX and the full interglacial MIS19c. During the interglacial phase, warm and stable high SSTs are found with an average spring temperature of ~8 °C and of ~7 °C in the winter. During MIS 19b-a, the Site U1314 seasonal SST profiles are characterized by three minima of temperatures corresponding to the stadial events of MIS 19 b-a (Fig. 3h-i). At Sites U1385 and U1314, the MIS 19 b-a interstadials are characterized by SSTs close to those of MIS 19c.

4. Discussion

4.1. Late MIS 20 and deglaciation (Termination IX)

The interval from ~805 to 787.5 ka predates the onset of the MIS 19 full interglacial conditions and represents the latter part of MIS 20 and the MIS 20/19 deglaciation phase (TIX) (Fig. 4). The SST record indicates that the Iberian Margin remained relatively warm until 794 ka (Fig. 3e-g) influenced by a continuous flow of the AzC as suggested by the presence of *G. ruber* (Fig. 4d) and *T. truncatulinoides* (Fig. 4e), in agreement with the findings of Martin-Garcia et al. (2018). The *G. inflata* (Fig. 4f) relative abundance record also confirms the evidence of a persistent warm glacial thermocline off Iberia during most of MIS 20 as suggested by Bahr et al. (2018). The drop in the abundance of planktonic foraminifera taxa associated with the AzC (Fig. 4 d - f), the increase in *N. pachyderma* (Fig. 4b) and the drop in SSTs of about 8 °C (Fig. 3e) marks the beginning of the terminal stadial event at ~794 ka characterized by a reduction of deep water ventilation as supported by a contemporaneous decrease in benthic $\delta^{13}C$ values (Fig. 3b) (Hodell et al., 2015, 2022). This event is also clearly identified by the shift towards low values of log (Ca/Ti) and high Zr/Sr ratios (Hodell et al., 2013, 2015, 2022) (Fig. 3c). The log (Ca/Ti) variations reflect relative changes in biogenic carbonate in the sediment; high values of biogenic carbonate are recorded during interglacial and interstadial phases resulting in high log (Ca/Ti) values, while the ratio decreases during glacial and stadial periods (Hodell et al., 2013, 2015, 2022).

At the Site U1385, distinct variations in the abundance patterns of planktonic foraminifera assemblages indicate that the terminal stadial was not a homogenous period but was punctuated by three short-term changes in the sea surface circulation, as discussed below.

During the first phase labeled 'a' (794–788 ka), high abundances of polar *N. pachyderma* (Fig. 4b) and a sharp decline in *G. ruber* and *T. truncatulinoides* (Fig. 4 d-e) indicate a pronounced cooling of the Iberian Margin region because of the southward shift of the subpolar front. These changes are concomitant with the increase in iceberg discharges in the subpolar North Atlantic, as recorded at Site U1314 (Hernandez-Almeida et al., 2012) (Fig. 4k). *N. pachyderma* is the dominant planktonic foraminifera species during Heinrich events in the North Atlantic

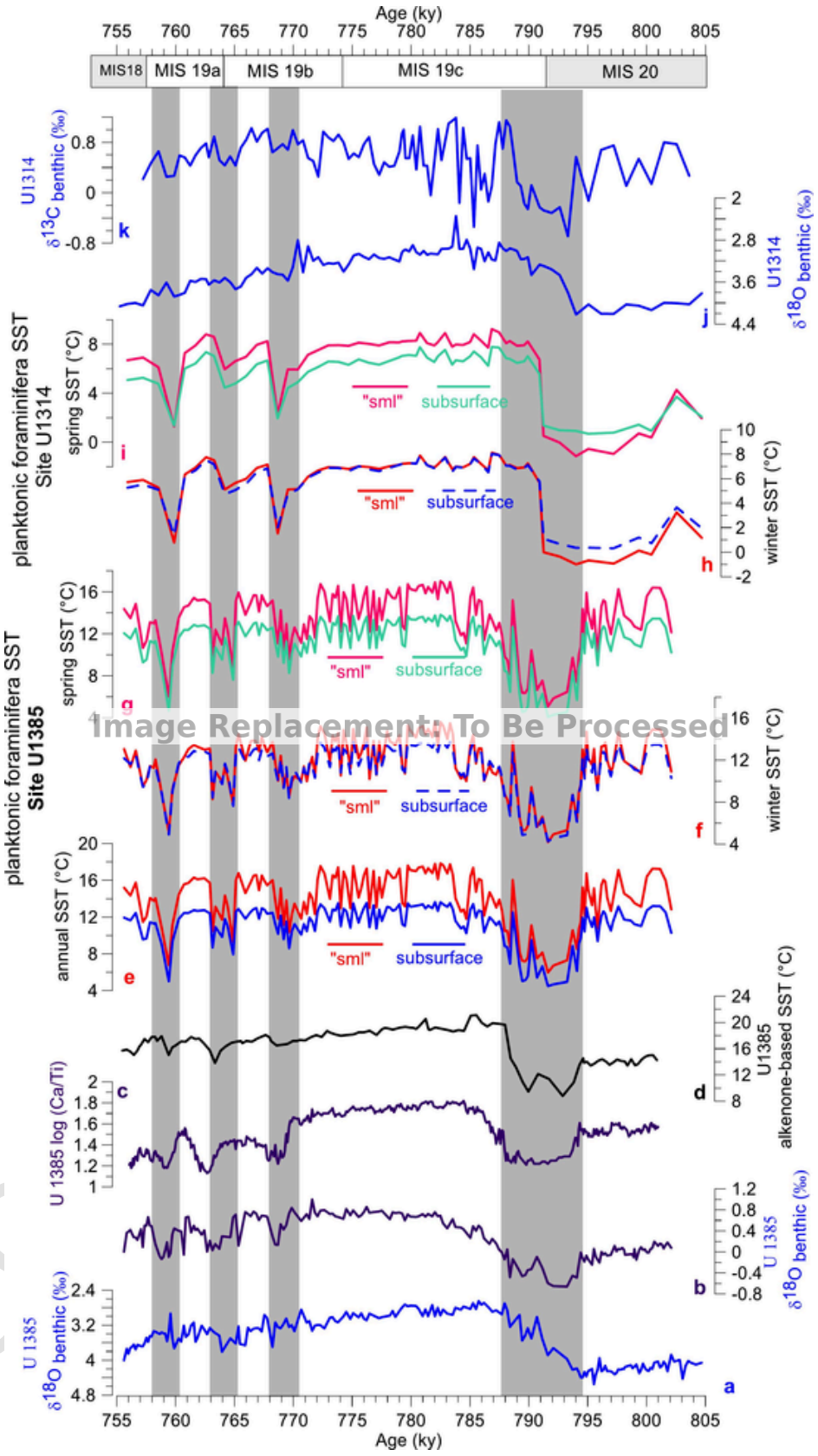

Fig. 3. Faunal-based Sea Surface Temperatures at IODP Site U1385 and Site U1314 through MIS 20 and MIS 19 compared with geochemical data from the same sites and alkenone and pollen data from the Site U1385. (a) Benthic $\delta^{18}O$ record at Site U1385 (Hodell et al., 2015; Sánchez Goñi et al., 2016). (b) Benthic $\delta^{13}C$ record at IODP Site U1385 (Hodell et al., 2015; Sánchez Goñi et al., 2016). (c) log (Ca/Ti) record at IODP Site U1385 (Hodell et al., 2015). (d) Alkenone-based SST

curve at IODP Site U1385 (Rodrigues et al., 2017). (e-g) Annual and seasonal SST at Site U1385 at surface mixed layer (sml) and subsurface sea water. (h-i) seasonal SST at IODP Site U1314 at surface mixed layer (sml) and subsurface sea water. (j) Benthic $\delta^{18}O$ record at Site U1314 (Alonso-Garcia et al., 2011b; Hernandez-Almeida et al., 2012). (k) Benthic $\delta^{13}C$ record at Site U1314. Light grey bands highlight stadial phases. Dark grey band highlight MIS 20 terminal stadial. Light yellow band indicates the climate optimum according to the planktonic foraminifera assemblages. Light pink band indicates warming event during terminal stadial. Dark pink band indicates warming Event 1. Light blue band highlights Event 2, the cold event preceding the full interglacial conditions. (For interpretation of the references to colour in this figure legend, the reader is referred to the web version of this article.)

Ocean (Heinrich, 1988; Bond et al., 1992), and it is considered to be a tracer of the southward penetration of cold and fresh water masses driven by north Atlantic iceberg discharge events (e.g. Bond et al., 1992). During the middle-late Pleistocene, peaks in *N. pachyderma* abundance in sediment cores from the Iberian Margin (Cayre et al., 1999; de Abreu et al., 2003; Parente et al., 2004; Vautravers and Shackleton, 2006; Eynaud et al., 2009; Marino et al., 2014; Martin-Garcia et al., 2015; Naughton et al., 2016) have been also related to north Atlantic iceberg discharges. The arrival of extremely cold and low salinity water at the Iberian Margin is also supported by the concomitant drop of the sea-surface and subsurface temperatures (Fig. 3e-g) and the abrupt increase in the percentages of alkenone $C_{37:4}$ at Site U1385 (Rodrigues et al., 2017) (Fig. 4c). This extreme cooling led to a decreased influence of the AzC and the warmer north Atlantic Transitional Water to the southern Iberian Margin as suggested by the drop in the relative abundances of *G. inflata* (Fig. 4f) and *G. ruber* (Fig. 4d). The maximum expansion of semi-desert plants recorded during this cold interval (Fig. 4g, Sánchez Goñi et al., 2016) indicates reduced heat and moisture transport towards Iberia and colder and drier climate conditions on land. This fact has been linked to a deflection of the westerly winds due to the atmospheric changes associated with the southward migration of the subpolar front and the slowdown of the AMOC driven by the ice sheet discharges during the terminal stadial event.

At ~790.2 ka, a short-term increase in *G. inflata* (Fig. 4f) occurred during a time of increasing insolation (Fig. 4n), which may indicate a warming as suggested by the concomitant relative rise in foraminifera- and alkenone-based SST records (Fig. 3d; 3e-g) and drop in *N. pachyderma* and $C_{37:4}$ relative abundances (Fig. 4 b-c). This may indicate a temporary interruption in the arrival of polar waters to the Iberian Margin during the terminal stadial event related to short-term northward shift of subpolar front. During this short relative warming event, labeled "phase b", the AzC seems to play a minor role as indicated by very low abundances of *T. truncatulinoides* and *G. ruber,* suggesting a southernmost position of the AzF. A sharp, very short-lived increase of the polar species (Fig. 4b) concomitant with an abrupt increase of $C_{37:4}$ at about 789.7 ka (Fig. 4 c) and a further cooling of about 4 °C in SST record (Fig. 3e), marks the last phase of terminal stadial (phase c) and indicates a renewed intrusion of meltwaters into the region during a persistent cold and arid climate period on land (Sánchez Goñi et al., 2016). The high abundance of semi-desert taxa in the pollen assemblages from Site U1385 (Fig. 4g) corroborates this interpretation (Sánchez Goñi et al., 2016) suggesting that the region was not under the influence of the westerly wind belt that usually transports moisture to the Atlantic margin of the Iberian Peninsula.

During TIX, further support for the interpretation of subpolar meltwater intrusion in the North Atlantic at high and middle latitudes comes from increases in Si/Sr at IODP Site U1308 (Fig. 4m) (Hodell et al., 2008) and from $C_{37:4}$ alkenone and quartz abundance at IODP Site U1313 (Naafs et al., 2011). Those records indicate the input of silicate-rich Ice Rafted Detritus (IRD) from North Atlantic and European ice sheets with crystalline bedrock and the occurrence of iceberg melting at least as far south as 41°N (Naafs et al., 2011). However, the absence of detrital carbonate at this time suggests there was no Heinrich event sensu stricto (Hemming, 2004) associated with TIX (Hodell et al., 2008). The cold terminal stadial event recorded prior to TIX at Site U1385 and in the wider North Atlantic was probably related to the destabilization of the European Ice sheets as suggested by Rodrigues et al. (2017).

At 788.4 ka, a rapid increase of *G. ruber* and *T. truncatulinoides* (Fig. 4d, e) indicates that during TIX the cold conditions of the terminal stadial were followed by a warming event, labeled as "Event 1". This event is characterized by a strong rise of sea surface temperatures of about 8 °C (Fig. 3 e) indicating a renewed influence of the AzC offshore Portugal. At this time, a very short recovery of Mediterranean forest pollen at the expense of semi-desert communities (Fig. 4g) suggests a weak increase of temperature and humidity on land (Sánchez Goñi et al., 2016). The prominent warming was suddenly interrupted by a new cooling event as indicated by the drop of about 7 °C in the sea surface temperatures, and of about 5 °C in the subsurface temperatures (Fig. 3 e-g) and by a sharp increase of *N. pachyderma* (light blue bar in Fig. 4b) and a drop of *G. ruber* abundance values. This cooling event, labeled as "Event 2", seems to correspond to a 1000-yr-long cooling event on land as indicated by a renewed expansion of semi-desert communities in the pollen assemblages at about 787.5 ka (Fig. 4g), which preceded the onset of the full interglacial conditions (Tajo interglacial) (Sánchez Goñi et al., 2016). This event could be associated with a very short-term cold spell recognized in the western and central Mediterranean Sea, before the interglacial warming inception, during TIX (Maiorano et al., 2016; Trotta et al., 2019; Marino et al., 2020; Quivelli et al., 2021). Similar cold and dry events occurring at TIX have been also observed in lacustrine successions from central Italy (Giaccio et al., 2015). The planktonic foraminifera and pollen assemblage fluctuations recognized at Site U1385 during TIX are closely related and highlight the contemporaneity and strong coupling of regional hydrological and atmospheric changes.

4.1.1. *Evolution of meridional thermal gradient during MIS20 and Termination IX*

Before the onset of MIS 20 terminal stadial, the SST records indicate relatively warm conditions along the Iberian Margin in contrast with rather low temperatures reconstructed at Site U1314 (Fig. 3e-i) suggesting that the Arctic Front was located at a latitude south of Site U1314. The relative warm conditions at Site U1385 indicate that the site was under the influence of the AzC, as indicated by the foraminifera assemblages and by the high thermal gradient (Fig. 4h-i). Therefore, NAC was diverted southeastwards preventing the arrival of warm waters to the subpolar North Atlantic. However, at ODP Site 980, located eastwards of Site U1314, the *N. pachyderma* abundance values (Fig. 4 l) remained low during part of the glacial phase as a consequence of the eastwards deflection of the NAC, resulting in a delay in cooling because of the gradual south-eastward migration of the AF during the mid-Pleistocene glacial stages (Alonso-Garcia et al., 2011b; Barker et al., 2021).

At Site U1314 winter and spring subsurface seawater temperatures indicate slightly warmer conditions than on the surface (Fig. 3h-i). Hernández-Almeida et al. (2015) also observed higher subsurface temperatures during times of IRD deposition using trace metal analyses (Mg/Ca) of planktonic foraminifera during episodes of weak AMOC. The accumulation of subsurface warming, during ice-rafting events at northern latitudes, is related to the development of a halocline that creates an inverse thermocline with cold waters on top and warm water from the NAC underneath (Hernández-Almeida et al., 2015). With the onset of terminal stadial, the thermal gradient between Sites U1314 and U1385 was reduced because of the arrival of cold water along the Iberian Margin and the reduced influence of the AzC. The first warming phase occurring during the terminal stadial event at Site U1385, labeled phase b in Fig. 3, corresponds to an abrupt rise in surface and sub-

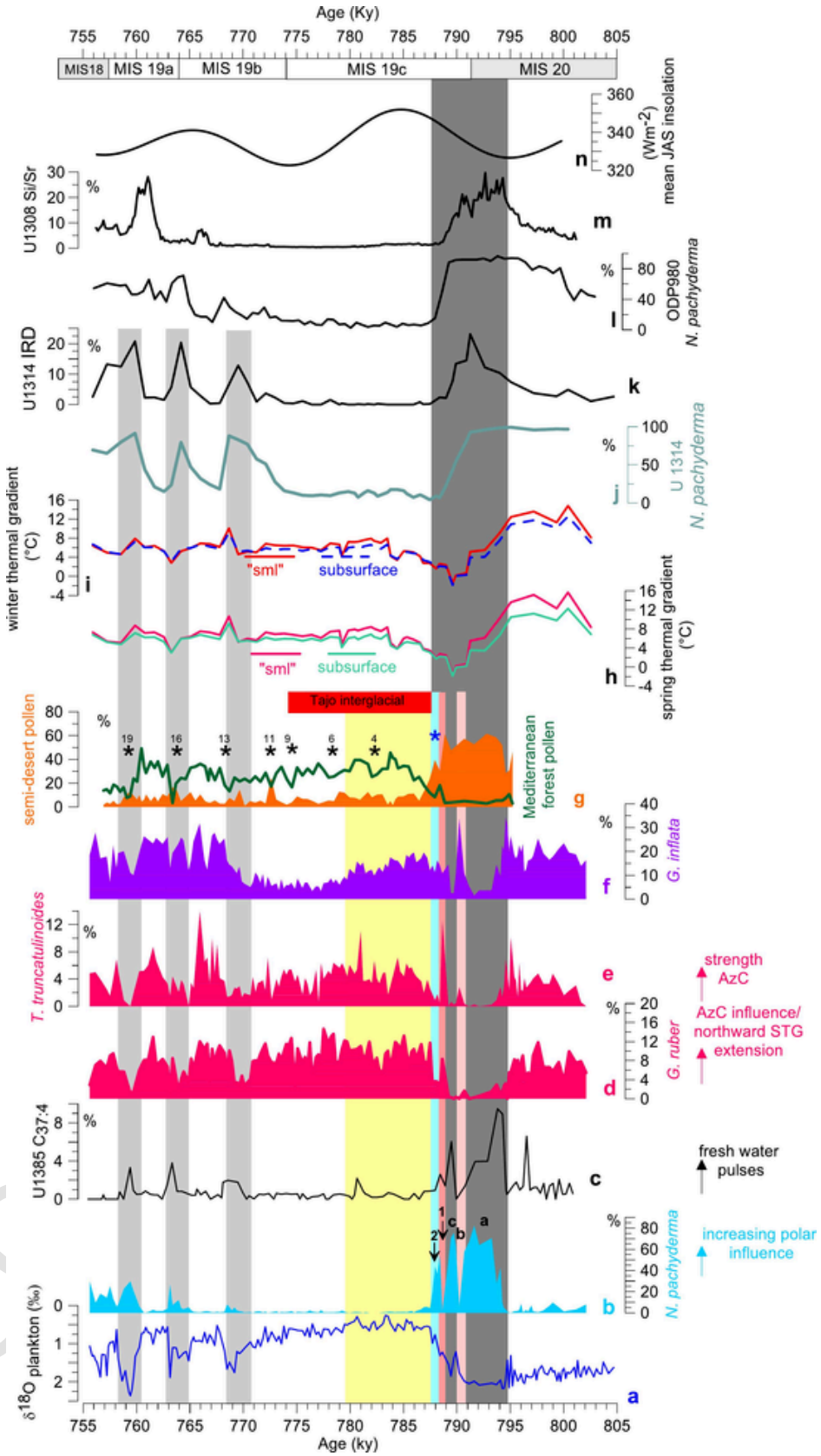

Fig. 4. Climate and paleoceanographic phases trough MIS 20 and MIS 19 at IODP Site U1385 based on planktonic foraminiferal proxies. (a) Planktonic $\delta^{18}O$ record at Site U1385 (Hodell et al., 2015; Sánchez Goñi et al., 2016). (b) Abundance pattern of *N. pachyderma* at Site U1385. (c) $C_{37:4}$ based freshwater pulse record at IODP Site U1385 (Rodrigues et al., 2017). (d-e) Abundance patterns of planktonic foraminifera species (*G. ruber* and *T. trucatulinoides*) related to AzC and STG. (f)

Abundance pattern of *G. inflata* at Site U1385. (g) pollen taxa abundances relevant for the climate variability on land (Sánchez Goñi et al., 2016). (h-i) Seasonal thermal gradient between IODP Site U1385 and IODP Site U1314. (j) Abundance pattern of *N. pachyderma* at IODP Site U1314 (Alonso-Garcia et al., 2011b; Hernández-Almeida et al., 2013). (k) IRD fluxes from Site U1314 (Alonso-Garcia et al., 2011b; Hernandez-Almeida et al., 2012). (l) Abundance pattern of *N. pachyderma* at Site 980 (Wright and Flower, 2002). (m) Si/Sr record at IODP Site U1308 (Hodell et al., 2008). (n) Mean summer insolation (JAS) (65° N) from Laskar et al. (2004). Light grey bands highlight stadial phases. Dark grey band highlight MIS 20 terminal stadial. Light yellow band indicates the climate optimum according to the planktonic foraminifera assemblages. Light pink band indicates warming event during terminal stadial. Dark pink band indicates warming Event 1. Light blue band highlights Event 2, the cold event preceding the full interglacial conditions. Black asterisks indicate Mediterranean forest contractions (the numeration of these events is according to Sánchez Goñi et al., 2016), blue asterisk indicates the cooling event before the onset of the Tajo interglacial according to Sánchez Goñi et al., 2016. (For interpretation of the references to colour in this figure legend, the reader is referred to the web version of this article.)

surface SST at Site U1314 (Fig. 3h- i) and a minimum thermal gradient between the Iberian Margin and high-latitude North Atlantic. The warming phase was accompanied by a progressive increase of benthic $\delta^{13}C$ values (Fig. 3k) suggesting improved deep-water ventilation and strengthening of the NAC that transports heat northward to the location of Site U1314, thereby leading to a lower north-south thermal gradient (Fig. 4h-i). During TIX, the simultaneous increase of benthic $\delta^{13}C$ values at Site U1385 and U1314 (Fig. 3b, k) during the warming phase b and Event 1 indicates that the increasing influence of the warmer AzC to the Portuguese Margin was accompanied by an increase in deep water ventilation in the North Atlantic probably related to strengthening of the AMOC. The prominent increase of AzC-related fauna (*T. truncatulinoides* and *G. ruber*) during Event 1 compared to previous warm phase suggests lower rates of meltwater released to the ocean, as the deglaciation progressed, causing a higher northward heat transport and displacement of the STG. At Site U1314, the drop of *N. pachyderma* abundances (Fig. 4j) is further evidence of the northern position of the polar front at this time while the increased abundances of *G. inflata* (Fig. 5j) indicate the increasing influence of warm-temperate transitional water at high latitudes.

4.2. MIS 19 and full interglacial conditions

The beginning of full interglacial conditions, at 787.5 ka is marked by the reactivation of the AzC that persisted throughout all of MIS 19c, and interstadials including those that occur on the MIS 19b-a as indicated by high abundances of *G. ruber* (Fig. 4d). In agreement with the patterns of planktonic $\delta^{18}O$ and log (Ca/Ti) (Fig. 3a, c), the increase of wwt in the foraminifera assemblages seems to be the response to the arrival of warm waters (Fig. 5c) and high sea surface temperatures to the Iberian Margin (Fig. 5b). On land the full interglacial, named Tajo interglacial, is defined as the interval of highest forest expansion with maximum abundances of Mediterranean forest sclerophyllous taxa (Fig. 5i), suggesting the establishment of Mediterranean climate conditions characterized by marked seasonality (warm and dry summers and wet winters) (Sánchez Goñi et al., 2016).

Between 787.5 ka and ~ 780 ka the co-occurrence of high abundance of wwt (Fig. 5c) and the presence of *T. sacculifer* (Fig. 5d) defines an interval with persistent seasonal low-nutrient and predominantly stratified surface water conditions (Salgueiro et al., 2008, 2010). The high abundances of wwt together with *G. inflata* (Fig. 5e) could be related to the strengthening of the AzC and the increase in the influence of warm transitional water masses that flow north of the Azores where *G. inflata* proliferates. The maximum expansion of Mediterranean forest component on land clearly is indicative of higher winter precipitation which indicates increased influence of the westerly wind systems in SW Iberia and related southward winter position of AH. Such conditions led to moderate surface-water stratification, resulting in a prolonged warming of surface waters promoted by the long-term intensified influence of water masses of subtropical origin along the Iberian Margin probably guaranteed by intensified influence of the winter IPC and ENACWst. The lower abundance of *N. incompta* (Fig. 5f) during this interval indicates a weak influence of the colder PC in agreement with findings based on calcareous nannofossil assemblages at Site U1313, which indicate the arrival of warmer waters up to 41°N (Emanuele et al., 2015). The highest surface and subsurface temperatures (Fig. 3h-i) and the highest abundances of *G. inflata* recorded at Site U1314 (Fig. 5j) concur to indicate that early MIS19c was the warmest interval of the substage when warm NAC prevailed at high latitudes. The occurrence of *G. bulloides* (Fig. 5h) in the assemblages at IODP Site U1385 indicates that seasonal wind-induced mixing episodes occurred during this warm interval.

During the older interval of MIS19c (787.5 ka – 780 ka) the occurrence of *T. quinqueloba,* indicative of cold and high fertility environments, could also be associated with the seasonal mixing as this species can proliferate during upwelling conditions (Sautter and Sancetta, 1992; Schiebel et al., 2004; Davis et al., 2016; Hernández-Almeida et al., 2011). At about 784.5 ka, high abundances of *T. quinqueloba* result in a prominent drop of temperatures of about 5 °C in the annual and seasonal SST records (Fig. 3e-g) with a minimum of sea surface annual temperature of about 13 °C (Event 3 in Fig. 5). These increases of *T. quinqueloba* coincide with the maximum expansion of the Mediterranean forest indicative of the establishment of marked seasonal climate conditions on land characterized by warm and dry summers and wet winters (Sánchez Goñi et al., 2016). We cannot exclude that the seasonal fertilization related to continental nutrient input during winter precipitation on land increased the abundance of *T. quinqueloba*, during MIS 19c, in accordance with the ecological affinities of the species (Bartels-Jónsdóttir et al., 2015; Jonkers et al., 2010; Rohling et al., 1997).

4.2.1. Air-sea interaction during interglacial MIS 19c

During MIS 20 terminal stadial and TIX, as discussed above, the planktonic foraminifera assemblages and SST records from IODP Site U1385 document millennial scale climate fluctuations (Fig. 4b-g) that clearly coupled the climate variations recorded on land by pollen assemblages evidencing a strongly interaction between ocean and atmosphere systems and North Atlantic climate and oceanographic changes.

At IODP Site U1385, Sánchez Goñi et al. (2016) found that MIS 19 was punctuated by forest contraction episodes indicative of millennial-scale cooling and drying conditions in southwestern Iberia during the maximum forested phase as consequence of the reinforcement and northward shift of the westerlies during winter. Unexpectedly, the foraminifera-based SST record does not register any temperature drop (Fig. 5b) concomitant with the cooling events recorded on land during MIS 19c probably related to high northward heat transport guaranteed by active AzC and northward displacement of the STG at this time. Alkenone-based SST during the interglacial interval at Site U1385 (Sánchez Goñi et al., 2016) also shows quite stable and warm conditions during the full interglacial interval (Sánchez Goñi et al., 2016) suggesting a land-ocean decoupling (Sánchez Goñi et al., 2016). The cold land–warm ocean decoupling at millennial-scale indicates repeated periods of intensified northward transport of heat from equatorial regions and associated water vapor triggered by precession-forced low latitude climate changes (Ferretti et al., 2015; Sánchez Goñi et al., 2016). This moisture increase, during the decrease of summer insolation, could have contributed to growth of the ice sheet during the onset of MIS 18 (Sánchez Goñi et al., 2016).

The decoupling of SST with land dynamics that are closely related to atmospheric processes suggests that SST was influenced by oceano-

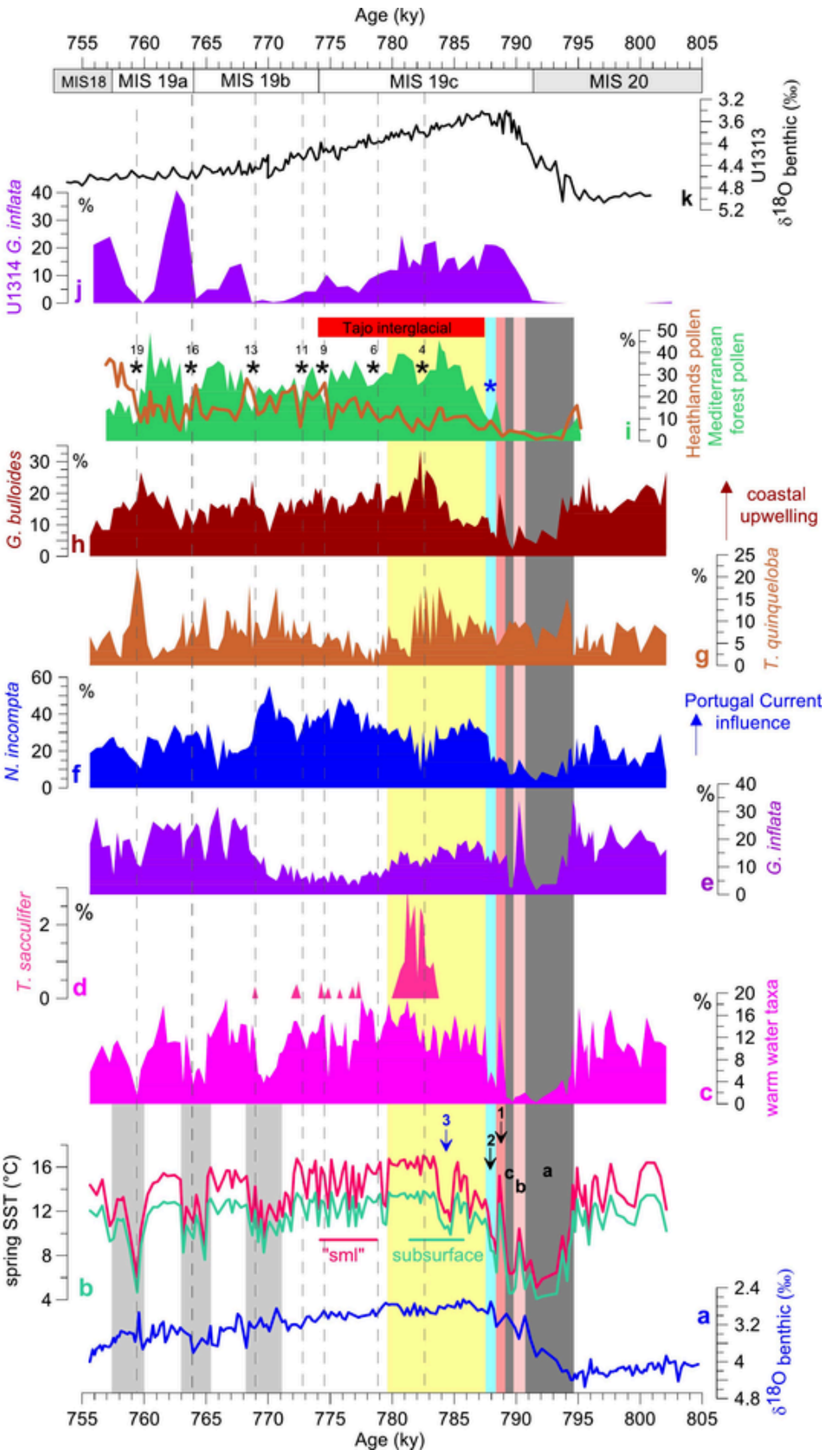

Fig. 5. Climate and paleoceanographic phases trough MIS 20 and MIS 19 at IODP Site U1385 based on planktonic foraminiferal proxies. (a) Benthic $\delta^{18}O$ record at Site U1385 (Hodell et al., 2015; Sánchez Goñi et al., 2016). (b) Spring SST at Site U1385 at surface mixed layer (sml) and subsurface sea water. (c-h) Abundance patterns of selected planktonic foraminifera species at IODP Site U1385. (i) Mediterranean forest pollen taxa (green line) and Heathlands (brown line) (Sánchez Goñi et

al., 2016). (j) Abundance pattern of *G. inflata* at IODP Site U1314 (Alonso-Garcia et al., 2011b; Hernández-Almeida et al., 2013). (k) Benthic $\delta^{18}O$ record at IODP Site U1313 (Ferretti et al., 2015). Light grey bands highlight stadial phases. Dark grey band highlight MIS 20 terminal stadial. Light pink band indicates warming phase c during terminal stadial. Dark pink band indicates warming Event 1. Light blue band highlights Event 2, the cold event preceding the full interglacial conditions. Blue arrow indicates Event 3, the cooling event during MIS19c according to planktonic foraminifera-based SST. Black asterisks indicate Mediterranean forest contractions (the numeration of these events is according to Sánchez Goñi et al., 2016) and dashed lines their correlation with major drop in wwt assemblages. Blue asterisk indicates the cooling event before the onset of the Tajo interglacial according to Sánchez Goñi et al., 2016. (For interpretation of the references to colour in this figure legend, the reader is referred to the web version of this article).

graphic processes rather than atmospheric dynamics. However, planktonic foraminifera assemblages may also be affected by atmospheric processes through changes in wind-induced surface ocean mixing. During MIS 19c, the reduction of wwt concomitant with the events on land could be an ecological response of these taxa to eutrophication episodes caused by a larger wind-induced mixing season related to drought and cooler temperatures in southwestern Iberia during winter. The high abundances of *G. bulloides* during the forest contraction event 4 (782 ka) and event 6 (778 ka) (black asterisks in Fig. 5i) support this hypothesis. *G. bulloides* is considered the main component of the planktonic foraminifera assemblage associated with upwelling conditions in this region (Salgueiro et al., 2008) and during these events it shows the highest abundances (Fig. 5h) throughout the full interglacial interval. Higher wind activity in spring-summer would have facilitated the destabilization of the water column and intensified sea water mixing as consequence of diminished influence of the winter westerlies in Iberia. The intensified mixing conditions lead to higher concentration of nutrient in the sea waters, thereby inhibiting the proliferation of warm and oligotrophic taxa. The SST remain high because, at this time, the AzC is active, and the site is under the influence of ENACWst. The occurrence of the tropical taxon *T. sacculifer* during this time interval further supports the interpretation of persistently warm SSTs.

4.3. Late MIS 19 and glacial inception

From ~780 ka onwards, the annual and seasonal temperatures at Site U1385 show a large variability and a drop of average temperatures of about 1.5–1 °C (Fig. 3). In the assemblages, a gradual decrease occurs in the abundance of *G. inflata* (Fig. 5e) that is accompanied by an increase in *N. incompta* (Fig. 5f), further indicating cooler temperatures. *N. incompta* is the major component of the PC assemblage along the Iberian Margin today (Salgueiro et al., 2008), with the highest abundances north of 39°N where the water temperature is colder than in the south year-round (Salgueiro et al., 2008). At Site U1385, cooler temperatures favored the replacement of *G. inflata* by *N. incompta* because the PC brought cold nutrient-rich water from the northern latitudes. The increase in percentages of heathlands pollen indicates the establishment of a cool and less seasonal climate regime on land characterized by more homogeneously distributed precipitation over the year with cooler and higher rainfall during the summer (Sánchez Goñi et al., 2016). Evidence of more persistent cool and nutrient-rich waters are also found at Site U1313, where the presence of these waters has been related to the intensification of the cooler NAC forced by variations in high-latitude summer insolation (Emanuele et al., 2015). From ~780 ka onwards, the drop in the abundances of *G. inflata* in the assemblages (Fig. 5j), at site U1314, could also be related to the NAC. Cooler climate conditions are also recorded in the western Mediterranean basin starting from ~778 ka, as suggested by calcareous plankton and pollen assemblages (Toti et al., 2020).

The increase of *N. incompta* and benthic $\delta^{18}O$ values during late MIS 19c, in combination with the decrease of alkenone-based (Fig. 3d) (Rodrigues et al., 2017) and foraminifera-based temperatures (Fig. 3e-g) at IODP Site U1385 is interpreted as a change in the climate regime in the southern Iberian Margin, probably related to ice sheet expansion at high latitude. The slight increase of *N. pachyderma* abundances at ODP Site 980 (Fig. 4l) starting at ~780 ka further supports the onset of progressive cooling that affects the entire North Atlantic. However, the AzC was still seasonally influencing the Iberian Margin because the high abundance of *G. ruber* (Fig. 4d) indicates seasonal transport of warm, salty waters to the site and the high percentages of *G. bulloides* indicates wind-driven mixing and enhanced productivity (Fig. 5h). These data support an increase in the meridional thermal gradient that coincides with the maximum $\delta^{13}C$, reflecting a vigorous deep water ventilation and the arrival of moisture to the high northern latitudes, which in turn started building-up the ice sheets at the MIS 19c/b transition (~775 ka).

From about 771 ka, the wwt abundance record (Fig. 5c) shows high frequency variability corresponding to stadial-interstadial oscillations that are in good agreement with the oscillations in the planktonic $\delta^{18}O$ curve (Fig. 5a) and with the log (Ca/Ti) record during MIS 19b-a (Fig. 3b). The stadials are characterized by reductions in wwt abundances and drops in planktonic foraminifera-based (Fig. 3e-g) and alkenone-based SSTs (Fig. 3d) (Rodrigues et al., 2017) suggesting cooling of surface and subsurface waters. The first of those stadial events occurred between 771 ka and 769 ka as recorded by the increase of *N. incompta*, *T. quinqueloba* (Fig. 5f-g) and *N. pachyderma* (Fig. 4b) and the sharp decrease of wwt (Fig. 5c), indicating a sustained influence of cold water transported by the PC. The drop in *G. ruber* (Fig. 4d) abundances suggests a diminished influence of the AzC at Site U1385 related to a southern displacement of AzF. This interpretation is supported by the temperature drop at Site U1314 (Fig. 3h-i). The records from North Atlantic Site U1313 also support a southward migration of the NAC and consequent increase in the influence of cooler waters at this time (Emanuele et al., 2015). The gradual increase in abundances of polar *N. pachyderma* during the subsequent stadials of MIS 19b-a is indicative of a progressive southward influence of subpolar water and it is consistent with the *N. pachyderma* abundance record at the ODP Site 980 (Fig. 4l) and at Site U1314 (Fig. 4j) which suggest that the subpolar front rapidly oscillated from its southward position during the stadials to northward positions during the interstadials. At Site U1385 this change is also supported by the trends of lower SST (Fig. 3e-g) and higher $C_{37:4}$ values (Fig. 4c) while, on land, the Mediterranean forest reductions along with semi-desert community expansions (Fig. 4g) suggest a shift towards colder and drier winter episodes more severe than those detected during MIS19c (Sánchez Goñi et al., 2016). The low north-south thermal gradient (Fig. 4h-i) suggests that the ice discharges in the North Atlantic and the related meltwater affected both the subpolar gyre and Iberian Margin and, therefore, the SSTs became more similar across different latitudes.

The interstadials were marked by a sudden rise of annual and seasonal SST that show values very close to those recorded during MIS 19c (Fig. 3e-g). The prominent increase in the abundance of *G. ruber* and *T. truncatulinoides* (Fig. 4d, e) indicates an intensification of the STG and AzC in this sector of the Iberian Margin which played a major role in warming the sea surface, while seasonal mixing favored the proliferation of *G. bulloides*. Interstadial climate conditions were comparable with the Tajo interglacial phase both in the sea and on land where the pollen assemblages indicate the establishment of Mediterranean climate related to a greater influence of the westerlies that bring moisture to the Iberian Margin (Sánchez Goñi et al., 2016). Overall, the climate variability during MIS 19b-a along the Iberian Margin is a response to repeated shifts of westerlies along with the relative position of the AzF and Polar Front. These findings are consistent with the climate patterns in the North Atlantic (Channell et al., 2010; Kleiven et al., 2011;

Tzedakis et al., 2012a, 2012b; Emanuele et al., 2015; Ferretti et al., 2015; Sánchez Goñi et al., 2016; Alonso-Garcia et al., 2011a, 2011b), Antarctic EDC ice core record (Jouzel et al., 2007; Pol et al., 2010), and with the millennial-scale climate oscillation recorded in western and central Mediterranean sites (Maiorano et al., 2016; Nomade et al., 2019; Marino et al., 2020; Toti et al., 2020) and in lacustrine sediments from central Italy (Giaccio et al., 2015; Regattieri et al., 2019) during MIS 19a-b.

Our findings indicate that during the MIS 19/18 transition, the Iberian Margin experienced the influence of cooler water related to progressive southern migration of subpolar front. This reconstruction is consistent with the increasing trend of benthic $\delta^{18}O$ values at IODP Site U1385, accounting for both colder deep sea water temperatures and continental ice sheet growth. Evidence of the progressive southern migration of the Polar Front is also indicated by the increasing trend of *N. pachyderma* and benthic $\delta^{18}O$ at Site U1314. An increase in the global ice volume starting from late MIS 19c and culminating in the onset of glacial MIS 18 is also supported by a similar trend of benthic $\delta^{18}O$ at IODP Site U1313 (Fig. 5k) (Ferretti et al., 2015).

5. Conclusion

The analysis of planktonic foraminifera from the Iberian Margin IODP Site U1385 allow us to document orbital and millennial-scale paleoceanographic and climate changes during MIS 20 and MIS 19. These changes were mainly controlled by shifts of the AzF and Polar Front as indicated by the faunal and stable isotope records. The combination of planktonic foraminifera and available pollen data from the same site permitted the identification of the role of atmospheric versus marine processes in these changes.

During MIS 20, the expanded ice sheets resulted in a strong cooling in the SPG whereas the Iberian Margin remained relatively warm under the influence of the AzC. During the TIX terminal stadial event (between 794 ka and 789 ka), fluctuating pulses of cold and fresh water during iceberg discharges into the North Atlantic lowered the sea surface and subsurface temperatures at the Iberian Margin at the same time as the establishment of cold, arid climate conditions on land. The establishment of full interglacial conditions during MIS 19c was preceded by short-term fluctuations in AzC assemblages and SSTs resulting in successive warming/cooling phases in the ocean coupled with warming/cooling events on land. Between 787.5 and 780 ka, the greater influence of the southern AzC and warm transitional waters define the climatic optimum of MIS 19c. During this interval, the foraminifera-based SST shows a decoupling with the climate changes recorded on land by pollen assemblages. On land, several cool and dry millennial-scale events are recorded but the foraminifera-based SST records indicate almost stable annual and seasonal warm temperatures guaranteed by the arrival of warm water of subtropical origin at the Iberian Margin. Thus, the planktonic foraminifera climate proxies indicate that during the interglacial phase the SSTs were dominated by oceanographic rather than atmospheric processes, supporting the land-ocean decoupling inferred from pollen and alkenone-based SSTs at Site U1385. However, planktonic foraminifer assemblages show variations in key species related to wind-induced surface ocean mixing that allowed us to track the millennial-scale events recorded on land with the pollen assemblages. During the cool and dry millennial-scale events on land, greater wind activity in spring-summer would have caused an intensification in seasonal mixing as indicated by increased abundances of *G. bulloides* during a time of relatively high SST when the site was under the influence of the AzC. The repeated northward transport of heat from lower to high latitude and increase moisture flux during cold conditions on land could have contributed to growth the ice sheets at the onset of MIS 18. The full interglacial conditions started to deteriorate at ~780 ka when *N. incompta* abundance increases at the expense of *G. inflata,* indicating cooler SSTs and the establishment of a cool, less seasonal climate regime on land. The MIS 19 b-a interval was characterized by high frequency variability corresponding to stadial-interstadial oscillations related to shifts of the polar and subtropical fronts coupled with warm-wet/cold-arid climate oscillations on land. From the glacial inception (MIS 19c/b towards MIS18) a cooling trend along the Iberian Margin indicates the progressive southward migration of the polar front, supported by the gradual increase of *N. pachyderma* and *T. quinqueloba*. During these stadial events the SST gradient was reduced because the ice discharges affected both the SPG and Iberian Margin and the SST became more similar across latitudes.

Supplementary data to this article can be found online at https://doi.org/10.1016/j.palaeo.2023.111450.

Uncited references

Declaration of Competing Interest

The authors declare that they have no known competing financial interests or personal relationships that could have appeared to influence the work reported in this paper.

Data availability

Data will be made available on request.

Acknowledgements

The authors thank the Integrated Ocean Drilling Program for providing samples. This research was financially supported by MIUR [Fondi FFABR Angela Girone] and benefited from instrumental upgrades from "Potenziamento Strutturale PONa3_00369 dell'Università degli Studi di Bari, Laboratorio per lo Sviluppo Integrato delle Scienze e delle Tecnologie dei Materiali Avanzati e per dispositivi innovativi (SISTEMA). MAG and FJS acknowledge funding from MCIN/AEI (grants RTI2018-099489-B-I00 and PID2021-128322NB-I00) and FCT (grant PTDC/CTA-GEO/29897/2017 - WARMWORLDS). The authors thank two anonymous reviewers for cconstructive comments and suggestions that improved the quality of this study.

References

Aksu, A.E., Hiscott, R.N., Kaminski, M.A., et al., 2002. Last glacial–Holocene paleoceanography of the Black Sea and Marmara Sea: stable isotopic, foraminiferal and coccolith evidence. Mar. Geol. 190 (1–2), 119–149.

Alonso-Garcia, M., Sierro, F.J., Kucera, M., Flores, J.A., Cacho, I., Andersen, N., 2011a. Ocean circulation, ice sheet growth and interhemispheric coupling of millennial climate variability during the mid-Pleistocene (ca 800–400 ka). Quat. Sci. Rev. 30, 3234–3247.

Alonso-Garcia, M., Sierro, F.J., Flores, J.A., 2011b. Arctic front shifts in the subpolar North Atlantic during the Mid-Pleistocene (800–400 ka) and their implications for ocean circulation. Palaeogeogr. Palaeoclimatol. Palaeoecol. 311, 268–280.

André, A., Weiner, A., Quillévéré, F., Aurahs, R., Morard, R., Douady, C.J., de Garidel-Thoron, T., Escarguel, G., de Vargas, C., Kucera, M., 2013. The cryptic and the apparent reversed: lack of genetic differentiation within the morphologically diverse plexus of the planktonic foraminifer *Globigerinoides sacculifer*. Paleobiology 39 (1), 21–39.

Bahr, A., Kaboth, S., Hodell, D., Zeeden, C., Fiebig, J., Friedrich, O., 2018. Oceanic heat pulses fueling moisture transport towards continental Europe across the mid-Pleistocene transition. Quat. Sci. Rev. 179, 48–58.

Barker, S., Zhang, X., Jonkers, L., Lordsmith, S., Conn, S., Knorr, G., 2021. Strengthening Atlantic inflow across the mid-Pleistocene transition. Paleoceanogr. Paleoclimatol. 36. https://doi.org/10.1029/2020PA004200. . e2020PA004200.

Bartels-Jónsdóttir, H.B., Voelker, A.H.L., Abrantes, F.G., Salgueiro, E., Rodrigues, T., Knudsen, K.L., 2015. High-frequency surface water changes in the Tagus prodelta off Lisbon, eastern North Atlantic, during the last two millennia. Mar. Micropaleontol. 117, 13–24.

Barton, E., Inall, M., Sherwin, T., Torres, R., 2001. Vertical structure, turbulent mixing and fluxes during Lagrangian observations of an upwelling filament system off Northwest Iberia. Prog. Oceanogr. 51, 249–267. https://doi.org/10.1016/s0079-6611(01)00069-6.

Bé, A.W.H., 1977. An ecological, zoogeographic and taxonomic review of recent planktonic foraminifera. In: Ramsay, A.T.S. (Ed.), Oceanic Micropaleontology. Academic, San Diego, California, pp. 1–100.

Bé, A.W.H., Tolderlund, D.S., 1971. Distribution and ecology of living planktonic foraminifera in surface waters of the Atlantic and Indian Oceans. In: Funnel, B.M., Riedel, W.R. (Eds.), The Micropaleontology of Oceans. Cambridge University Press, New York, pp. 105–149.

Berger, A., Loutre, M.F., Mélice, J.L., 2006. Equatorial insolation: from precession harmonics to eccentricity frequencies. Clim. Past 2, 131–136. https://doi.org/10.5194/cp-2-131-2006.

Bertini, A., Toti, F., Marino, M., Ciaranfi, N., 2015. Vegetation and climate across the Early- Middle Pleistocene transition at the Montalbano Jonico section (southern Italy). Quat. Int. 383, 74e88.

Bond, G., Heinrich, H., Broecker, W., Labeyrie, L., McManus, J., Andrews, J., Houn, S., Jantschik, R., Clasen, S., Simet, C., Tedesco, K., Klas, M., Bonani, G., Ivi, S., 1992. Evidence for massive discharges of icebergs into the North Atlantic Ocean during the last glacial period. Nature 360 (6401), 245–249.

Cayre, O., Lancelot, Y., Vincent, E., Hall, M.A., 1999. Paleoceanographic reconstructions from planktonic foraminifera offthe Iberian Margin: temperature, salinity, and Heinrich events. Paleoceanography 14 (3), 384–396.

Channell, J.E.T., Hodell, D.A., Singer, B.S., Xuan, C., 2010. Reconciling astrochronological and 40Ar/39Ar ages for the Matuyama-Brunhes boundary in the late Matuyama Chron. Geochem. Geophys. Geosyst. 11, Q0AA12. https://doi.org/10.1029/2010GC003203.

Chapman, M.R., Maslin, M.A., 1999. Low-latitude forcing of meridional temperature and salinity gradients in the subpolar North Atlantic and the growth of glacial ice sheets. Geology 27, 875–878.

Conkright, M.E., Locarnini, R.A., Garcia, H.E., O'Brien, T.D., Boyer, T.P., Stephens, C., Antonov, J.I., 2002. World Ocean Atlas 2001: Objective Analyses, Data Statistics, and figures: CD-ROM documentation.

Darling, K.F., Kucera, M., Kroon, D., Wade, C.M., 2006. A resolution for the coiling direction paradox in Neogloboquadrina pachyderma. Paleoceanography 21 (2), PA2011.

Davis, C.V., Hill, T.M., Russell, A.D., Gaylord, B., Jahncke, J., 2016. Seasonality in planktic foraminifera of the central California coastal upwelling region. Biogeosciences 13, 5139–5150. https://doi.org/10.5194/bg-13-5139-2016.

de Abreu, L., Shackleton, N.J., Schönfeld, J., Hall, M.A., Chapman, M., 2003. Millennial-scale oceanic climate variability off the western Iberian Margin during the last two glacial periods. Mar. Geol. 196, 1–20.

Emanuele, D., Ferretti, P., Palumbo, E., Amore, F.O., 2015. Sea-surface dynamics and palaeoenvironmental changes in the North Atlantic Ocean (IODP Site U1313) during Marine Isotope Stage 19 inferred from coccolithophore assemblages. Palaeogeogr. Palaeoclimatol. Palaeoecol. 430, 104–117.

Eynaud, F., de Abreu, L., Voelker, A., Schönfeld, J., Salgueiro, E., Turon, J.L., Penaud, A., Toucanne, S., Naughton, F., Sánchez Goñi, M.F., Malaizé, B., Cacho, I., 2009. Position of the Polar Front along the western Iberian Margin during key cold episodes of the last 45 ka. Geochem. Geophys. Geosyst. 10, Q07U05. https://doi.org/10.1029/2009GC002398.

Ferretti, P., Crowhurst, S.J., Hall, M.A., Cacho, I., 2010. North Atlantic millennial-scale climate variability 910 to 790 ka and the role of the equatorial insolation forcing. Earth Planet. Sci. Lett. 293, 28e41. https://doi.org/10.1016/j.epsl.2010.02.016.

Ferretti, P., Crowhurst, S.J., Naafs, B.D.A., Barbante, C., 2015. The marine isotope stage 19 in the mid-latitude North Atlantic Ocean: astronomical signature and intra-interglacial variability. Quat. Sci. Rev. 108. https://doi.org/10.1016/j.quascirev.2014.10.024.

Fiúza, A.F.G., 1984. Hidrologia e dinámica das águas costeiras de Portugal (Ph.D. thesis). Univ. of Lisbon, Lisbon.

Fiúza, A., Macedo, M., Guerreiro, M., 1982. Climatological space and time variation of the Portuguese coastal upwelling. Oceanol. Acta 5, 31–40.

Fiúza, A.F.G., Hamann, M., Ambar, I., Díaz del Río, G., González, N., Cabanas, J.M., 1998. Water masses and their circulation off western Iberia during May 1993. Deep-Sea Res. I Oceanogr. Res. Pap. 45, 1127–1160.

Frouin, R., Fiúza, A., Ambar, I., Boyd, T.J., 1990. Observations of a poleward surface current off the coasts of Portugal and Spain during the winter. J. Geophys. Res. 95, 679–691.

Giaccio, B., Regattieri, E., Zanchetta, G., Nomade, S., Renne, P.R., Sprain, C.J., Drysdale, R.N., Tzedakis, P.C., Messina, P., Scardia, G., Sposato, A., Bassinot, F., 2015. Duration and dynamics of the best orbital analogue to the present interglacial. Geology 43, 603–606. https://doi.org/10.1130/G36677.1.

Giraudeau, J., 1993. Planktonic foraminiferal assemblages in surface sediments from the southwest African margin. Mar. Geol. 110, 47–62.

Girone, A., Capotondi, L., Ciaranfi, N., Di Leo, P., Lirer, F., Maiorano, P., Marino, M., Pelosi, N., Pulice, I., 2013. Paleoenvironmental change at the lower Pleistocene Montalbano Jonico section (southern Italy): global versus regional signals. Palaeogeogr. Palaeoclimatol. Palaeoecol. 371, 62–79.

Gould, W.J., 1985. Physical oceanography of the Azores front. Prog. Oceanogr. 14, 167–190. https://doi.org/10.1016/0079-6611(85)90010-2.

Haynes, R., Barton, E.D., 1990. A polewardflow along the Atlantic coast of the Iberian Peninsula. J. Geophys. Res. 95, 11425–11442.

Heinrich, H., 1988. Origin and consequences of cyclic ice rafting in the northeast Atlantic Ocean during the past 130,000 years. Quat. Res. 29, 142–152.

Hemleben, C., Spindler, M., Anderson, O.R., 1989. Modern Planktonic Foraminifera. Springer, New York, pp. 1–363.

Hemleben, C., Spindler, M., Anderson, O.R., 1989. Modern Planktonic Foraminifera. Springer-Verlag, New York, p. 363.

Hemming, S.R., 2004. Heinrich events: massive late Pleistocene detritus layers of the North Atlantic and their global climate imprint. Rev. Geophys. 42. https://doi.org/10.1029/2003RG000128. . RG1005.

Hernández-Almeida, I., Bárcena, M.A., Flores, J.A., Sanchez-Vidal, A., Calafat, A., 2011. Microplankton response to environmental conditions in the Alboran Sea (Western Mediterranean): one year sediment trap record. Mar. Micropaleontol. 78 (1–2), 14–24.

Hernandez-Almeida, I., Sierro, F.J., Cacho, I., Flores, J.A., 2012. Impact of suborbital climate changes in the North Atlantic on ice sheet dynamics at the Mid-Pleistocene transition. Paleoceanography 27, PA3214.

Hernández-Almeida, I., Sierro, F.J., Flores, J.A., Cacho, I., Filippelli, G.M., 2013. Palaeoceanographic changes in the North Atlantic during the M id-P leistocene T ransition (MIS 31–19) as inferred from planktonic foraminiferal and calcium carbonate records. Boreas 42 (1), 140–159.

Hernández-Almeida, I., Sierro, F.-J., Cacho, I., Flores, J.-A., 2015. Subsurface North Atlantic warming as a trigger of rapid cooling events: evidences from the Early Pleistocene (MIS 31–19). Clim. Past 11 (4), 687–696.

Hijmans, R.J., 2017. raster: Geographic Data Analysis and Modeling, Rpackage version 2.6–7. available at: https://CRAN.R-project.org/package=rasterhttps://CRAN.R-project.org/package=raster. (last access: 12 May 2019).

Hodell, D.A., Channell, J.E.T., Curtis, J.H., Romero, O.E., Röhl, U., 2008. Onset of "Hudson Strait" Heinrich events in the eastern North Atlantic at the end of the middle Pleistocene transition (~640 ka)? Paleoceanography 23, PA4218. https://doi.org/10.1029/2008PA001591.

Hodell, D., Crowhurst, S., Skinner, L., Tzedakis, P.C., Margari, V., Channell, J.E.T., Kamenov, G., Maclachlan, S., Rothwell, G., 2013. Response of Iberian Margin sediments to orbital and suborbital forcing over the past 420 ka. Paleoceanography 28 (1), 185–199. https://doi.org/10.1002/palo.20017.

Hodell, D., Lourens, L., Crowhurst, S., Konijnendijk, T., Tjallingii, R., Jiménez-Espejo, F., Skinner, L., Tzedakis, P.C., the Shackleton Site Project Members, 2015. A reference time scale for site U1385 (Shackleton site) on the SW Iberian Margin. Glob. Planet. Chang. 133, 49–64.

Hodell, D., Crowhurst, S., Lourens, L., Margari, V., Nicolson, J., Rolfe, J.E., Skinner, L.C., Thomas, N., Tzedakis, P.C., Mleneck-Vautravers, M.J., Wolff, E.W., 2022. A 1.5-Million-Year Record of Orbital and Millennial Climate Variability in the North Atlantic, Clim. Past Discuss. [preprint]. https://doi.org/10.5194/cp-2022–61in review.

Johannessen, T., Jansen, E., Flatoy, A., Ravelo, A.C., 1994. The relationship between surface water masses, oceanographic fronts and paleoclimatic proxies in surface sediments of the Greenland, Iceland, Norwegian seas. In: Zahn, R., et al. (Ed.), NATO ASI Series 117. Springer-Verlag, New York, pp. 61–85.

Jonkers, L., Moros, M., Prins, M.A., Dokken, T., Dahl, C.A., Dijkstra, N., Perner, K., Brummer, G.J.A., 2010. A reconstruction of sea surface warming in the northern North Atlantic during MIS 3 ice-rafting events. Quat. Sci. Rev. 29 (15–16), 1791–1800.

Jouzel, J., Masson-Delmotte, V., Cattani, O., Dreyfus, G., Falourd, S., Hoffmann, G., Minster, B., Nouet, J., Barnola, J.M., Chappellaz, J., Fischer, H., Gallet, J.C., Johnsen, S., Leuenberger, M., Loulergue, L., Luethi, D., Oerter, H., Parrenin, F., Raisbeck, G., Raynaud, D., Schilt, A., Schwander, J., Selmo, E., Souchez, R., Spahni, R., Stauffer, B., Steffensen, J.P., Stenni, B., Stocker, T.F., Tison, J.L., Wener, M., Wolff, E.W., 2007. Orbital and millennial Antarctic climate variability over the past 800,000 years. Science 317, 793–796. https://doi.org/10.1126/science,1141038.

Juggins, S., 2017. Rioja: Analysis of Quaternary Science Data, R package version (0.9–15.1). available at: http://cran.r-project.org/package=riojahttp://cran.r-project.org/package=rioja. (last access: 12 May 2019), 2017.

Kaiser, E.A., Caldwell, A., Billups, K., 2019. North Atlantic upper-ocean hydrography during the mid-Pleistocene transition evidenced by *Globorotalia truncatulinoides* coiling ratios. Paleoceanogr. Paleoclimatol. 34, 658–671. https://doi.org/10.1029/2018PA003502.

Käse, R., Siedler, G., 1982. Meandering of the subtropical front south-east of the Azores. Nature 300, 245–246. https://doi.org/10.1038/300245a0.

Kleiven, H., Hall, I.R., McCave, I.N., Knorr, G., Jansen, E., 2011. North Atlantic coupled deep-water flow and climate variability in the middle Pleistocene. Geology 39 (4), 343–346.

Laskar, J., Robutel, P., Joutel, F., Gastineau, M., Correia, A.C.M., Levrard, B., 2004. A long term numerical solution for the insolation quantities of the Earth. Astron. Astrophys. 428, 261–285. https://doi.org/10.1051/0004-6361:20041335.

Maiorano, P., Bertini, A., Capolongo, D., Eramo, G., Gallicchio, S., Girone, A., Pinto, D., Toti, F., Ventruti, G., Marino, M., 2016. Climate signatures through the Marine Isotope Stage 19 in the Montalbano Jonico section (Southern Italy): a land-sea perspective. Palaeogeogr. Palaeoclimatol. Palaeoecol. 461, 341–361.

Marcott, S.A., Clark, P.U., Padman, L., Klinkhammer, G.P., Springer, S.R., Liu, Z., OttoBliesner, B.L., Carlson, A.E., Ungerer, A., Padman, J., He, F., Cheng, J., Schmittner, A., 2011. Ice-shelf collapse from subsurface warming as a trigger for Heinrich events. Proc. Nat. Acad. Sci. USA 108, 13415–13419.

Margaritelli, G., Vallefuoco, M., Di Rita, F., Capotondi, L., Bellucci, L.G., Insinga, D.D., Petrosino, S., Bonomo, I., Cacho, A., Cascella, L., Ferraro, L., Florindo, F., Lubritto, C., Lurcock, P.C., Magri, D., Pelosi, N., Rettori, R., Lirer, F., 2016. Marine response to climate changes during the lastfive millennia in the central Mediterranean Sea. Glob. Planet. Chang. 142, 53–72.

Marino, M., Maiorano, P., Tarantino, F., Voelker, A., Capotondi, L., Girone, A., Lirer, F., Flores, J.-A., Naafs, B.D.A., 2014. Coccolithophores as proxy of seawater changes at orbital- to-millennial scale during middle Pleistocene Marine Isotope Stages 14-9 in North Atlantic core MD01- 2446. Paleoceanography 29, PA002574.

Marino, M., Bertini, A., Ciaranfi, N., Aiello, G., Barra, D., Gallicchio, S., Girone, A., La Perna, R., Lirer, F., Maiorano, P., Petrosino, P., Toti, F., 2015. Paleoenvironmental and climatostratigraphic insights for Marine Isotope Stage 19 (Pleistocene) at the Montalbano Jonico section, South Italy. Quat. Int. 383, 104–115. https://doi.org/10.1016/j.quaint.2015.01.043.

Marino, M., Girone, A., Gallicchio, S., Herbert, T., Addante, M., Bazzicalupo, P., Quivelli,

O., Bassinot, F., Bertini, B., Nomade, S., Ciaranfi, N., Maiorano, P., 2020. Climate variability during MIS 20-18 as recorded by alkenone-SST and calcareous plankton in the Ionian Basin (Central Mediterranean). Palaeogeogr. Palaeoclimatol. Palaeoecol. 560. https://doi.org/10.1016/j.palaeo.2020.110027.

Martin-Garcia, G.M., Alonso-Garcia, M., Sierro, F.J., Hodell, D.A., Flores, J.A., 2015. Severe cooling episodes at the onset of deglaciations on the Southwestern Iberian Margin from MIS 21 to 13 (IODP site U1385). Glob. Planet. Chang. 135, 159–169.

Martin-Garcia, G.M., Sierro, F.J., Flores, J.A., Abrantes, F., 2018. Change in the North Atlantic circulation associated with the mid-Pleistocene transition. Clim. Past 14, 1639–1651. https://doi.org/10.5194/cp-14-1639-.

Martrat, B., Grimalt, J.O., Shackleton, N.J., de Abreu, L., Hutterli, M.A., Stocker, T.F., 2007. Four climate cycles of recurring deep and surface water destabilizations on the Iberian Margin. Science 317 (5837), 502–507. https://doi.org/10.1126/science.1101706.

McAyeal, D.R., 1993. Binge/purge oscillations of the Laurentide ice sheet as a cause of North Atlantic's Heinrich events. Paleoceanography 8, 775–784.

McCartney, M.S., Talley, L.D., 1982. The subpolar mode water of the North Atlantic Ocean. J. Phys. Oceanogr. 12, 1169–1188.

Naafs, B.D.A., Hefter, J., Ferretti, P., Stein, R., Haug, H., 2011. Sea surface temperatures did not control thefirst occurrence of Hudson Strait Heinrich Events during MIS 16. Paleoceanography 26, PA4201. https://doi.org/10.1029/2011PA002135.

Naughton, F., Sánchez Goñi, M.F., Rodrigues, T., Salgueiro, E., Costas, S., Desprat, S., Duprat, J., Michel, E., Rossignol, L., Zaragosi, S., Voelker, A.H.L., Abrantes, F., 2016. Climate variability across the last deglaciation in NW Iberia and its margin. Quat. Int. 414, 9–22.

Nomade, S., Bassinot, F., Marino, M., Simon, Q., Dewilde, F., Maiorano, P., Esguder, G., Blamart, D., Girone, A., Scao, V., Pereira, A., Toti, F., Bertini, A., Combourieu-Nebout, N., Peral, M., Bourles, D., Petrosino, P., Gallicchio, S., Ciaranfi, N., 2019. High-resolution foraminifer stable isotope record of MIS 19 at Montalbano Jonico, southern Italy: a window into Mediterranean climatic variability during a low-eccentricity interglacial. Quat. Sci. Rev. 205, 106–125.

Oksanen, J., Blanchet, F.G., Friendly, M., Kindt, R., Legendre, P., McGlinn, D., Minchin, P.R., O'Hara, R.B., Simpson, G.L., Solymos, P., Henry, M., Stevens, H., Szoecs, E., Wagner, H., 2018. vegan: Community Ecology Package. R package version 2.5–2. available at: https://CRAN.R-project.

Ottens, J.J., 1991. Planktic foraminifera as North Atlantic watermass indicators. Oceanol. Acta 14, 123–140.

Overpeck, J.T., Webb, III, T., Prentice, I.C., 1985. Quantitative interpretation of fossil pollen spectra: dissimilarity coefficients and the method of modern analogs. Quat. Res. 23, 87–108.

Parente, A., Cachão, M., Baumann, K.-H., de Abreu, L., Ferreira, J., 2004. Morphometry of Coccolithus pelagicuss.L. (Coccolithophore, Haptophyta) from offshore Portugal, during the last 200 kyr. Micropaleontology 50, 107–120.

Peliz, A., Dubert, J., Santos, A.M.P., Oliveira, P.B., Le Cann, B., 2005. Winter upper ocean circulation in the Western Iberian Basin—Fronts, Eddies and Poleward Flows: an overview. Deep-Sea Res. I52, 621–646.

Pflaumann, U., Sarnthein, M., Chapman, M., d'Abreu, L., Funnell, B., Huels, M., Kiefer, T., Maslin, M., Schulz, H., Swallow, J., van Kreveld, S., Vautravers, M., Vogelsang, E., Weinelt, M., 2003. Glacial North Atlantic: sea-surface conditions reconstructed by GLAMAP 2000. Paleoceanography 18, 1065. https://doi.org/10.1029/2002PA000774.

Pol, K., Masson Delmotte, V., Johnsen, S., Bigler, M., Cattani, O., Durand, G., Falourd, S., Jouzel, J., Minster, B., Parrenin, F., Ritz, C., Steen Larsen, C.H., Stenni, B., 2010. New MIS 19 EPICA Dome C high resolution deuterium data: hints for a problematic preservation of climate variability at sub-millennial scale in the"oldest ice". Earth Planet. Sci. Lett. 298, 95–103.

Prell, W., 1985. The stability of low-latitude sea-surface temperatures: an evaluation of CLIMAP reconstructions with emphasis on positive SST anomalies. Tech. Rep. TR 025. U.S. Department of Energy, Washington, DC.

Pujol, C., Vergnaud-Grazzini, C., 1995. Distribution patterns of live planktic foraminifers as related to regional hydrography and productive systems of the Mediterranean Sea. Mar. Micropaleontol. 25, 187–217.

Quivelli, O., Marino, M., Rodrigues, T., Girone, A., Maiorano, P., Bertini, A., Niccolini, G., Trotta, S., Bassinot, F., 2021. Multiproxy record of suborbital-scale climate changes in the Algero-Balearic Basin during late MIS 20 - Termination IX. Quat. Sci. Rev. 260, 106916. https://doi.org/10.1016/j.quascirev.2021.106916.

R Core Team, 2020. R: A Language and Environment for Statistical Computing. R Foundation for Statistical Computing, Vienna.

Rahmstorf, S., 1995. Bifurcations of the Atlantic thermohaline circulation in response to changes in the hydrological cycle. Nature 378 (6553), 145–149.

Regattieri, E., Giaccio, B., Mannella, G., Zanchetta, G., Nomade, S., Tognarelli, A., Perchiazzi, N., Vogel, H., Boschi, C., Neil, R.D., Wagner, B., Gemelli, M., Tzedakis, P., 2019. Frequency and dynamics of millennial-scale variability during Marine Isotope Stage 19: insights from the Sulmona Basin (Central Italy). Quat. Sci. Rev. 214, 28–43.

Relvas, P., Barton, E.D., Dubert, J., Oliveira, P.B., Peliz, A., Da Silva, J., Santos, A.M.P., 2007. Physical oceanography of the western Iberia ecosystem: latest views and challenges. Prog. Oceanogr. 74, 149–173. https://doi.org/10.1016/j.pocean.2007.04.021.

Rodrigues, T., Voelker, A.H.L., Grimalt, J.O., Abrantes, F., Naughton, F., 2011. Iberian Margin sea surface temperature during MIS15 to 9 (580–300 ka): glacial suborbital variability versus interglacial stability. Paleoceanography 26, 1–16. https://doi.org/10.1029/2010PA001927.

Rodrigues, T., Alonso-García, M., Hodell, D.A., Rufino, M., Naughton, F., Grimalt, J.O., Voelker, A.H.L., Abrantes, F., 2017. A 1-Ma record of sea surface temperature and extreme cooling events in the North Atlantic: a perspective from the Iberian Margin. Quat. Sci. Rev. 172, 118–130.

Rohling, E.J., Den Dulk, M., Pujol, C., Vergnaud-Grazzini, C., 1995. Abrupt hydrographic change in the Alboran Sea (western Mediterranean) around 8000 yrs BP. Deep-Sea Res. 42, 1609–1619.

Rohling, E.J., Jorissen, F.J., De Stigter, H.C., 1997. 200-year interruption of Holocene sapropel formation in the Adriatic Sea. J. Micropalaeontol. 16 (2), 97–108.

Ruddiman, W.F., McIntyre, A., 1984. Ice-age thermal response and climatic role of the surface Atlantic Ocean, 40 N to 63N. Geol. Soc. Am. B. 95, 381–396.

Salgueiro, E., Voelker, A., Abrantes, F., Meggers, Pflaumann, U., Loncaric, N., González-Álvarez, R., Oliveira, P., Bartels Jónsdóttir, H.B., Moreno, J., Wefer, G., 2008. Planktonic foraminifera from modern sediments reflect upwelling patterns off Iberia: insights from a regional transfer function. Mar. Micropaleontol. 66, 135–164.

Salgueiro, E., Voelker, A.H.L., de Abreu, L., Abrantes, F., Meggers, H., Wefer, G., 2010. Temperature and productivity changes off the western Iberian Margin during the last 150 ky, Quaternary Sci. Rev. 29, 680–695.

Sánchez Goñi, M.F., Rodrigues, T., Hodell, D.A., Polanco-Martínez, J.M., Alonso García, M., Hernandez-Almeida, I., Desprat, S., Ferretti, P., 2016. Tropicallydriven climate shifts in southwestern Europe during MIS 19, a low eccentricity interglacial. Earth Planet. Sci. Lett. 448, 81–93.

Sánchez, R.F., Relvas, P., 2003. Spring–summer climatological circulation in the upper layer in the region of cape St. Vincent, SW Portugal. ICES J. Mar. Sci. 60, 1232–1250.

Sautter, L.R., Sancetta, C., 1992. Seasonal associations of phytoplankton and planktic foraminifera in an upwelling region and their contribution to the seafloor. Mar. Micropaleontol. 18, 263–268.

Schiebel, R., Waniek, J., Zeltner, A., Alves, M., 2002a. Impact of the Azores Front on the distribution of planktic foraminifers, shelled gastropods, and coccolithophorids. Deep-Sea Res. Part II, 49(19), 4035–4050.

Schiebel, R., Schmuker, B., Alves, M., Hemleben, C., 2002b. Tracking the recent and late Pleistocene Azores front by the distribution of planktic foraminifers. J. Mar. Syst. 37 (1–3), 213–227.

Schiebel, R., Zeltner, A., Treppke, U.F., Waniek, J.J., Bollmann, J., Rixen, T., Hemleben, C., 2004. Distribution of diatoms, coccolithophores and planktic foraminifers along atrophic gradient during SW monsoon in the Arabian Sea. Mar. Micropaleontol. 51 (3–4), 345–371.

Schmitz, W.J., McCartney, M.S., 1993. On the North Atlantic circulation. Rev. Geophys. 31 (1), 29–49.

Siccha, M., Kucera, M., 2017. ForCenS, a curated database of planktonic foraminifera census counts in marine surface sediment samples. Sci. Data 4 (1), 1–12.

Sousa, F.M., Bricaud, A., 1992. Satellite-derived phytoplankton pigment structures in the Portuguese upwelling area. J. Geophys. Res. 97 (C7), 11343–11356.

Spezzaferri, S., Kucera, M., Pearson, P.N., Wade, B.S., Rappo, S., Poole, C.R., Morard, R., Stalder, C., 2015. Fossil and genetic evidence for the polyphyletic nature of the planktonic foraminifera "Globigerinoides", and description of the new genus Trilobatus. PLoS One 10 (5), e0128108. https://doi.org/10.1371/journal.pone.0128108.

Telford, R., 2019. Ggpalaeo: Ggplot2 Plots for Analogue and Rioja Packages.

Telford, R., Birks, H., 2009.: Evaluation of transfer functions in spatially structured environments, Quat. Sci. Rev., 28, 1309–1316, 2009.

Telford, R.J., Birks, H.J.B., 2011. A novel method for assessing the statistical significance of quantitative reconstructions inferred from biotic assemblages. Quat. Sci. Rev. 30 (9–10), 1272–1278.

Telford, R.J., Li, C., Kucera, M., 2013. Mismatch between the depth habitat of planktonic foraminifera and the calibration depth of SST transfer functions may bias reconstructions. Clim. Past 9 (859–870), 2013. https://doi.org/10.5194/cp-9-859-2013.

Toti, F., Bertini, A., Girone, A., Marino, M., Maiorano, P., Bassinot, F., CombourieuNebout, N., Nomade, S., Buccianti, A., 2020. Marine and terrestrial climate variability in the western Mediterranean Sea during marine isotope stages 20 and 19. Quat. Sci. Rev. 243. https://doi.org/10.1016/j.quascirev.2020.106486.

Trachsel, M., Telford, R.J., 2016. Technical note: estimating unbiased transfer-function performances in spatially structured environments. Clim. Past 12, 1215–1223. https://doi.org/10.5194/cp-12-1215-2016.

Triantaphyllou, M., Antonarakou, A., Dimiza, M., Anagnostou, C., 2010. Calcareous nannofossil and planktonic foraminiferal distributional patterns during deposition of sapropels S6, S5 and S1 in the Libyan Sea (Eastern Mediterranean). Geo-Mar. Lett. 30 (1), 1–13.

Trotta, S., Marino, M., Maiorano, P., Girone, A., 2019. Climate variability through MIS20-MIS 19 in core KC01B, Ionian Basin (central Mediterranean Sea). Alp. Med. Quat. 32 (2), 1–15. https://doi.org/10.26382/AMQ.2019.10.

Tzedakis, P.C., Raynaud, D., McManus, J.F., Berger, A., Brovkin, V., Kiefer, T., 2009. Interglacial diversity. Nat. Geosci. 2, 751–755.

Tzedakis, P.C., Channell, J.E.T., Hodell, D.A., Kleiven, H.F., Skinner, L.C., 2012a. Determining the natural length of the current interglacial. Nat. Geosci. 5, 1–4.

Tzedakis, P.C., Wolff, E.W., Skinner, L.C., Brovkin, V., Hodell, D.A., McManus, J.F., Raynaud, D., 2012b. Can we predict the duration of an interglacial? Clim. Past 8, 1–13.

Vaughan, I.P., Ormerod, S.J., 2005. The continuing challenges of testing species distribution models. J. Appl. Ecol. 42 (4), 720–730.

Vautravers, M.J., Shackleton, N.J., 2006. Centennial-scale surface hydrology off Portugal during marine isotope stage 3: insights from planktonic foraminiferal fauna variability. Paleoceanography 21, PA3004. https://doi.org/10.1029/2005PA001144.

Vautravers, M.J., Shackleton, N.J., Lopez-Martinez, C., Grimalt, J.O., 2004. Gulf Steam variability during marine isotope stage 3. Paleoeanography 19, PA2011. https://doi.org/10.1029/2003PA000966.

Voelker, A.H.L., de Abreu, L., 2013. A Review of Abrupt Climate Change Events in the Northeastern Atlantic Ocean (Iberian Margin): Latitudinal, Longitudinal, and Vertical Gradients, Abrupt Climate Change: Mechanisms, Patterns, and Impacts. American

Geophysical Union, p. 15e37.
Voelker, A.H.L., Rodrigues, T., Billups, K., Oppo, D.W., McManus, J.F., Stein, R., Hefter, J., Grimalt, J.O., 2010. Variations in mid-latitude North Atlantic surface water properties during the mid-Brunhes (MIS 9–14) and their implications for the thermohaline circulation. Clim. Past 6, 531–552.
Wagner, B., Vogel, H., Francke, A., et al., 2019. Mediterranean winter rainfall in phase with African monsoons during the past 1.36 million years. Nature 573, 256–260. https://doi.org/10.1038/s41586-019-1529-0Wickham, H., 2016. ggplot2: elegant graphics for data analysis, Springer, New York.
Weaver, P.P.E., Pujol, C., 1988. History of the laste deglaciation in the Alboran Sea (Western Mediterranean) and adjacent North Atlantic as revealed by coccolith floras. Palaeogeogr. Palaeoclimatol. Palaeoecol. 64, 35–42.
Wickham, H., 2016. *ggplot2: Elegant graphics for data analysis*, 2nd ed. Springer, New York, NY.
Wright, A.K., Flower, B.P., 2002. Surface and deep ocean circulation in subpolar North Atlantic during the mid-Pleistocene revolution. Paleoceanography 17, 1068. https://doi.org/10.1029/2002PA000782.
Yin, Q.Z., Berger, A., 2012. Individual contribution of insolation and CO2 to the interglacial climates of the past 800,000 years. Clim. Dyn. 38, 709–724.
Yin, Q.Z., Berger, A., 2015. Interglacial analogues of the Holocene and its natural near future. Quat. Sci. Rev. 120, 28–46.
Expedition 339 Scientists, 2013. Site U1385. In: Stow, D.A.V., Hernández-Molina, F.J., Alvarez Zarikian, C.A., the Expedition 339 Scientists (Eds.), Proc. IODP 339. Integrated Ocean Drilling Program Management International, Inc., Tokyo.http://dx.doi.org/10. 2204/iodp.proc.339.103.2013
Pingree, R.D., Sinha, B., 1998. Dynamic topography (ERS-1/2 and seatruth) ofSubtropical ring (STORM 0) in the STORM corridor (32–341N, eastern basin, North Atlantic Ocean). Journal ofMarine Biological Association ofthe United Kingdom 78, 351–376.